Chapter 2
Pituitary Anatomy and Development

Ronald M. Lechan, Knarik Arkun, and Roberto Toni

Historical Anatomy

The most ancient suggestion of a pituitary gland in man can be traced to the Tantra Yoga, elaborated by the pre-Aryan, Dravidic culture and Aryan Brahmanic, Ayurvedic medicine of fifteenth to fifth centuries B.C. [1]. Although Vedic medical doctrine prohibited dissection of human cadavers, it recognized an "energy center" in the brain called ājñā chakra in ancient Sanskrit, believed to regulate consciousness and perception of "self." This center was symbolized by two petals of the lotus flower, reminiscent of the two thalamic masses [2], and, possibly, the two lobes of the pituitary gland [1]. According to the Tantric anatomy, this region included numerous efferent channels (nerve fibers) called nadis [3], which we now recognize to contain the hypothalamic tuberoinfundibular system (for historical reviews, see [4–7]).

R. M. Lechan (✉)
Department of Medicine, Division of Endocrinology, Diabetes and Metabolism, Tufts Medical Center and Tufts University School of Medicine, Boston, MA, USA
e-mail: rlechan@tuftsmedicalcenter.org

K. Arkun
Department of Anatomic and Clinical Pathology, Tufts Medical Center and Tufts University School of Medicine, Boston, MA, USA

R. Toni
Department of Medicine and Surgery, Unit of Biomedical, Biotechnological, and Translational Sciences, Section of Human Anatomy, RE.MO.BIO.S. Lab, Parma, Italy

Center for Sport and Exercise Medicine (SEM), University of Parma School of Medicine, c/o Maggiore Hospital, Parma, Italy

Museum of Biomedicine and Historical Laboratory (BIOMED), University of Parma Museum Network System, Parma, Italy

Department of Medicine, Division of Endocrinology, Diabetes, and Metabolism, Tufts Medical Center and Tufts University School of Medicine, Boston, MA, USA

N. A. Tritos, A. Klibanski (eds.), *Prolactin Disorders*, Contemporary Endocrinology, https://doi.org/10.1007/978-3-030-11836-5_2

The first anatomical description of the pituitary gland on record, however, was during the second century A.D. by Galen of Pergamon. In *Anatomicae Administrationes*, he described a physical connection between the pituitary and infundibulum of the hypothalamic third ventricle and its association with a surrounding vascular network that he called "rete mirabilis." He proposed this unique, arterial structure had a key role in the regulation of body energy, sensation, and impulse, which he referred to as "vital and animal spirits." Galen was influenced by the ancient, Greek anatomist, Herophilus of Alexandria (third century B.C.), however, to whom he credited the discovery of the rete mirabilis [4, 5, 8, 9]. Although absent in humans, the rete mirabilis is a well-developed structure in a number of animal species (*Carnivora*, *Cetacea*, *Edentata*, *and Ungulata*) and equivalent to the suprahypophysial, circuminfundibular, and prechiasmal arteriolar-capillary plexus of man [4–6]. In *De Usu Partium*, the major treatise of Galenic physiology, the pituitary gland is described as a receptacle for brain "waste" in the form of mucus or phlegm (pituita in Latin) that accumulates in the third ventricle as a result of the "metabolism" of "body energy" at the level of the rete mirabilis. This material was proposed to drain along the hypothalamic infundibulum and "filtered" by the pituitary gland before exiting through the nasal cavities [4, 5]. Although now archaic in concept, it is of interest that evidence for brain paravascular channels that drain into sinus-associated dural lymphatics and perivenular lymphatics (so-called glymphatic system) have recently been described [8], re-energizing the Galenic concept of nasopharyngeal extracerebral transport of "metabolic impurities" from the central nervous system.

Galenic concepts dominated for several centuries as indicated by drawings of the pituitary gland and rete mirabilis by Leonardo da Vinci in 1508 (Fig. 2.1a, b), but he also provided the first detailed drawings of the anatomy of the human skull base. These included transverse and sagittal views of the cranial fossa, giving a detailed anatomical depiction of the association between the third ventricle/pituitary stalk and the cranial vault, facial bones, and nasal/oral cavities (Fig. 2.1c–e). During the same period, Johannes de' Ketam published the superficial cranial projection of somatesthesia (Fig. 2.1f) in *Man of Diseases* (1491), corresponding to the frontal area where hyperalgesia occurs with stretching of the diaphragma sellae, as with a pituitary macroadenoma that extends into the suprasellar cistern [9]. In 1511, Michelangelo Buonarroti painted the fresco, *Creation of Adam*, on the ceiling of the Sistine Chapel, believed to be the first depiction of the hypothalamic-pituitary region (Fig. 2.1g, h) [4, 5].

It was not until the sixteenth century, however, that Berengario da Carpi in *Isagoge Breves* first challenged the Galenic concept of the pituitary gland as a basin that filtered cerebral waste products, based on his work with human cadavers, and described the sphenoid sinus as a route to the sella turcica [4, 5]. Shortly thereafter, Andreas Vesalius in *Tabulae anatomicae sex* (1538) described the venous drainage from the cranial vault, which recapitulates what we now recognize as the inferior and superior petrosal and sphenoparietal sinuses (Fig. 2.2a), and although demonstrated that the rete mirabilis originates from the internal carotid artery, surrounds the pituitary fossa, and then widens symmetrically and superiorly to vascularize the

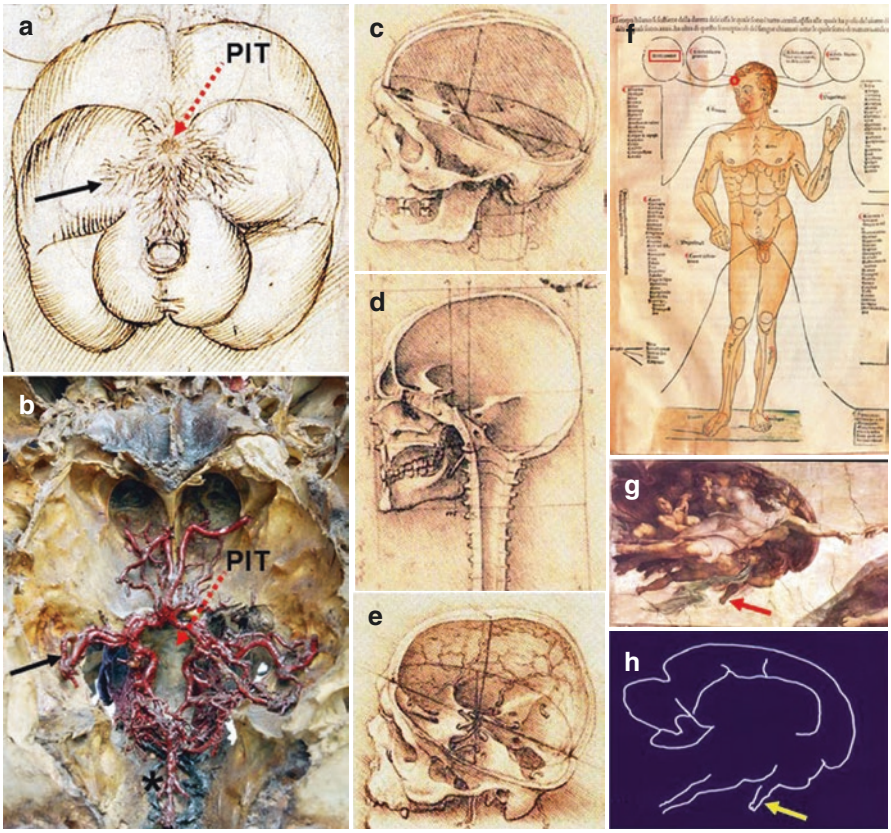

Fig. 2.1 (**a**) Drawing of the base of the brain by Leonardo da Vinci depicting the rete mirabilis (arrow) surrounding the pituitary gland (PIT), likely the oldest image of this anatomical region. Note squat morphology of the temporal lobes and width of the encephalic mass, typical of ox anatomy as opposed to human anatomy where an elongated morphology of brain lobes prevails and the rete mirabilis is absent. (Royal Library at Windsor Castle, Courtesy of the Historical Library of the Museum of Biomedicine – BIOMED, University of Parma, Parma, Italy, partly modified) (**b**) Injection-corrosion cast of the bovine rete mirabilis around the pituitary (PIT) fossa (dotted arrow) and basilar (asterisk) arteries. Note the arrangement of blood vessels around the sella turcica is very similar to that depicted by Leonardo in his drawing. (Courtesy of Prof. Ferdinando Gazza, nineteenth-century collection of the Museum of Veterinary Anatomy, University of Parma, Parma, Italy) (**c**–**e**) Drawings by Leonardo da Vinci of the middle cranial fossa, sella turcica, and their anatomical relationships with the cranial vault and facial bones. These drawings were the oldest anatomical maps inspiring the surgical and later stereotaxic approach to tumors of the hypothalamic-pituitary complex at the end of the nineteenth century. (**c**, **d**) From O'Malley and de C.M. Saunders [157]; (**e**) Royal Library at Windsor Castle, Courtesy of the Historical Library of the Museum of Biomedicine – BIOMED, University of Parma, Parma, Italy (**f**) Johannes de' Ketam's depiction of sensory afferent projections (*sensus communis*, red rectangle) in the median supraorbital, frontal region in *Man of Diseases*. (Modified from Premuda L. Storia dell'Iconografia Anatomica. Ciba Edizioni, Ciba-Geigy, 1993, ISBN 88-7645-107-2, p. 65.) (**g**) Detail from the fresco, Creation of Adam, by Michelangelo Buonarroti. Red arrow points to a limb of one of the angels. (**h**) Contour of fresco in (**g**) is reminiscent of a midline sagittal section of the human brain. Limb of the angel (yellow arrow) represents the pituitary stalk. ((**g**, **h**) Adapted from [158])

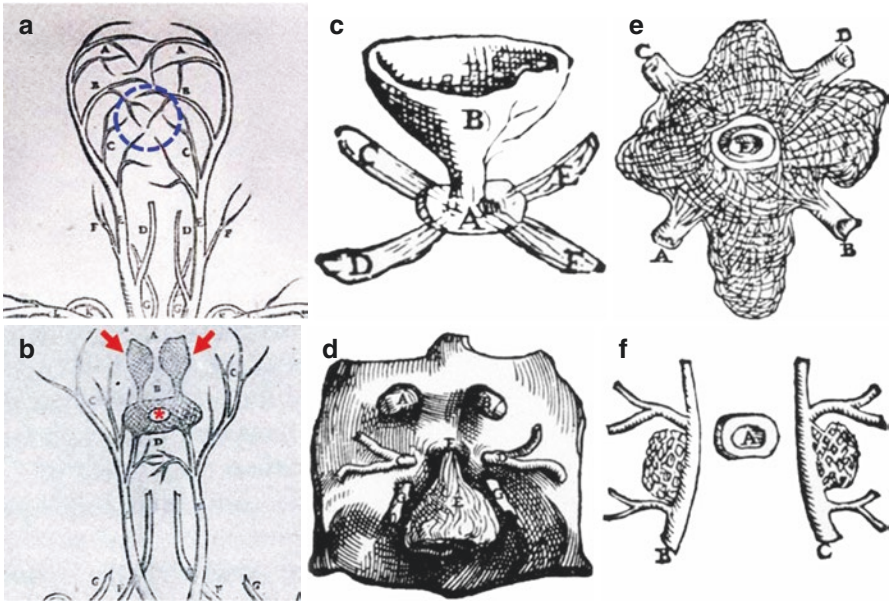

Fig. 2.2 Drawings of Andreas Vesalius. (**a**, **b**) Plates from *Tabulae anatomicae sex* depicting (**a**) anatomy of the venous vertebral and internal jugular systems and the common facial vein. Note the X-shaped, venous pattern at the center of the image (blue dotted circle) fed by six, symmetrical branches of the internal jugular vein reminiscent of the distribution of the inferior and superior petrosal and sphenoparietal sinuses around the cavernous sinus. (**b**) The arterial, vertebral (dorsal vessels) and common carotid (ventral vessels) systems. The rete mirabilis has central opening where the pituitary gland would be located (red asterisk) and fed by the internal carotid artery. Note that the *rete mirabilis* widens symmetrically and superiorly to vascularize the suprahypophysial, hypothalamic area (corresponding to the red arrowheads). (From [5, 9], partly modified.) (**c**–**f**) Plates from the seventh book of *De Humani Corporis Fabrica*. (**c**) Enlarged view of the pituitary (**A**) showing the hypothalamic infundibulum and ducts comprising the foramen lacerum and superior orbital fissure. (**d**) Anatomical relationships between the infundibulum (**e**), dural diaphragma sellae, internal carotid arteries, and oculomotor and optic nerves. (**e**) Enlarged view of the pituitary (**E**) surrounded by the *rete mirabilis* arising from branches of the internal carotid artery. (**f**) Detailed view of the association between the pituitary (**A**), carotid arteries, and rete mirabilis. (Partly modified from [5, 9]) (From the BIOMED Museum, University of Parma)

infundibulum and hypothalamic floor, he erroneously reported that it was present in man (Fig. 2.2b). Subsequently, in *De Humani Corporis Fabrica* (1543), he detailed the anatomical relationships between the pituitary gland and the hypothalamic infundibulum, diaphragma sellae, internal carotid arteries, and oculomotor nerves and, although now denying the presence of the rete mirabilis in man, held fast to the Galenic dogma by describing bony ducts of the cranial base he believed to drain brain mucus (Fig. 2.2c–f). The contemporary of Vesalius, Gabriele Fallopius,

similarly argued against the presence of the *rete mirabilis* in man, but it was not until the seventeenth century that Thomas Willis raised the possibility in *Cerebri Anatome* that "humors" from blood perfusing the ventral surface of the brain are carried to the pituitary gland, unwittingly anticipating current concepts of releasing and inhibiting factors for adenohypophysial regulation [4, 5]. The Galenic idea that the pituitary gland filters brain secretions into the nose was also criticized by Konrad Victor Schneider during the same period in *Liber Primus De Catarrhis* (1660), showing that the cribriform plate of the ethmoid bone was impervious to drainage from the central nervous system, and by Willis' assistant, Richard Lower, in his 1670 *Tractatus de Corde*, observing that the infundibular connection to the pituitary gland was filled with a gelatinous substance that would obstruct the possibility of mucous percolation from the third ventricle into the gland (see [6] for historical review).

Further advances were made in the eighteenth century by the French clinician and anatomist, Joseph Lieutaud, in *Essais Anatomique* (1742), who introduced the term "pituitary stalk" (la tige de la glande pituitaire) and described stalk vessels we now recognize as part of the portal circulation. In 1767, Luigi Galvani in *Disquisitiones Anatomicae Circa Membranam Pituitariam* showed that mucus passing through the nostrils originates from glands in the nasal mucosa and not the pituitary [10], and in 1791 Samuel Thomas von Sömmerring coined the term "hypophysis" in *Hirnlehre und Nervenlehre* [5]. However, it was not until the late in the nineteenth century and throughout the twentieth century that a new renaissance in the understanding the anatomy and importance of the pituitary gland was begun, coincident with the development of new and powerful histochemical and molecular techniques, and continues into the present century. Included was work by Santiago Ramón y Cajal in 1894 using the Golgi's silver impregnation technique to elucidate the connection between the hypothalamus and posterior pituitary (supraoptic-hypophysial tract), the discovery of hypothalamic neurosecretion by Ernst Scharrer in 1928, the finding by Popa and Fielding in 1930 of an interconnection between the pituitary and hypothalamus through the "hypophyseo-portal vessels" (although misinterpreted as blood flowing from the pituitary upward to the hypothalamus), evidence by Harris and Green between 1935 and 1955 that the blood flow in portal vessels was from the hypothalamic median eminence to the pars distalis of the pituitary gland and that electrical stimulation of the hypothalamus was ineffective in eliciting a pituitary response if the pituitary stalk was severed, and descriptions of the neurosecretory nature of the neurohypophysis by Wolfgang Bargmann in 1949 using the Gomori's histochemical method [11] (see also [6] for historical review). Many advancements have been made since, and those relevant to the current understanding of the anatomy of the pituitary gland are alluded to in the following sections. A timeline of major, historical breakthroughs in elucidation of the functional anatomy of the mammalian pituitary gland is summarized in Table 2.1.

Table 2.1 Timeline of major, historical breakthroughs in elucidation of the functional anatomy of the mammalian pituitary gland

1500–500 B.C	Tantric Yoga and Vedic medicine locate an energy center at the level of the thalamic-pituitary area	1791	Sömmerring introduces the term "hypophysis"
II century A.D	Galen describes the *rete mirabilis* around the pituitary considered a filter for brain mucous to the nasal cavities	1894	Santiago Ramón y Cajal describes the supraoptico-hypophysial tract in rats using the Golgi's silver impregnation method
1489–1511	Leonardo da Vinci and Michelangelo Buonarroti paint the pituitary gland, *rete mirabilis*, and possibly a brain section with the pituitary stalk	1928	Ernst Scharrer describes "glandular cells" in the fish hypothalamus (concept of "neurosecretion) using standard histologic techniques
1521–1523	Berengario da Carpi denies the existence of the *rete mirabilis*	1930	Popa and Fielding discover the pituitary portal system
1543	Andreas Vesalius publishes the drawings of the hypothalamic-pituitary unit, *rete mirabilis*, and pituitary venous drainage as currently known for petrosal sampling	1938	Feyrter identifies "clear cells" in the anterior pituitary using the tartaric acid-thionin staining as a marker of the diffuse endocrine system later described by AGE Pearse
1561	Gabriele Fallopius confirms the absence of the pituitary *rete mirabilis* in humans	1935–1955	Harris and Green demonstrate in anesthetized rats that blood in the portal vessels flows to the pituitary, and this vascular link is critical to the hypothalamic control of pituitary secretions
1664	Thomas Willis argues that humors out of the brain base may be carried to the pituitary gland	1949	Wolfgang Bargmann describes the posterior pituitary using the *Gomori's* chrome alum hematoxylin-phloxine *stain*
1660–1670	Schneider and Lower reject the Galenic idea that the pituitary gland filters brain secretions to the nose	1964	János Szentágothai defines the hypothalamic origin of the tuberoinfundibular tract in rats, and Kjell Fuxe shows its entire course using the Falck-Hillarp histochemical technique for monoamines
1742	Lieutaud discovers vessels in the pituitary stalk connected to those of the pituitary gland	1969–1970	Yoshimura et al. show that mice pituitary chromophobes may behave like pituitary stem cells, and Nakane provides ultrastructural bases for paracrine interactions in the pituitary gland
1767	Luigi Galvani shows that mucus passing through the nostrils originates from mucous glands of the human nasal mucosa and not from the pituitary gland	2009	Garcia-Lavandeira et al. identify stem cells/progenitors in the marginal zone of the adult human pituitary gland

Macroscopic Anatomy

Landmarks of the Sellar Region

The pituitary gland lies in the central part of the sella turcica (pituitary fossa), a saddle-shaped groove in the endocranial, superior surface of the sphenoid bone corresponding to the median part of the middle cranial fossa (Fig. 2.3a). On a lateral skull projection, the sella and pituitary lie 5–6 cm anterior to the point of the orthogonal intersection between Frankfurt horizontal plane and a vertical line descending from the vertex of the cranial vault (posterior to the bregma) to the center of the external acoustic meatus (Fig. 2.3b). Bordering the sella turcica is a bony thickening at the apex of its anterior wall, the tuberculum sellae, protruding upward as much as 3 mm to terminate into two, small, bony eminences, the middle clinoid process. Lateral and above are the anterior clinoid processes, forming the tip of the lesser wings of the sphenoid. The tuberculum sellae also forms the posterior wall of the chiasmatic groove into which rests the optic chiasm (Fig. 2.3a, c, d). Just above the optic chiasm are the anterior cerebral and anterior communicating arteries of the circle of Willis, the lamina terminalis, and third ventricle of the hypothalamus (Fig. 2.3d).

Lateral to the sella are the cavernous sinuses (Fig. 2.4a–c), a collection of spaces, loculated by fibrous septa between the outer periosteal and inner meningeal dural sheaths. The outer periosteal dural sheath covers the floor and anterior and posterior walls of the sella. The inner meningeal dura forms the lateral wall and roof of the cavernous sinus, gives rise to a very thin medial meningeal lining that serves as its medial wall and adheres to the capsule of the pituitary gland [12], and fuses with the cerebellar tentorium at the roof and superior aspects of the lateral walls of the sella turcica (Fig. 2.4c). Venous blood from the cavernous sinus (Fig. 2.4a) exits via endocranial tributaries of the internal jugular veins that include the superior and inferior petrosal sinuses and exocranial tributaries of the internal jugular vein, including the ophthalmic and facial veins.

Within the space between the medial and lateral walls of the cavernous sinus (Fig. 2.4a), a loose, reticular, connective tissue membrane envelops the oculomotor (III), trochlear (IV), abducens (VI), ophthalmic (V_1), and maxillary (V_2) branches of the trigeminal nerves and a sympathetic plexus that surrounds the internal carotid artery [12]. The internal carotid artery is separated from the pituitary gland by at least 2 mm but occasionally can indent the pituitary parenchyma. Once in the cavernous sinus, the internal carotid artery courses horizontally and anteriorly for ~2 cm (Fig. 2.4b–d), then forms a genu forward, and is fixed to either the anterior clinoid process by a dural ring (carotid collar) or between the anterior and middle clinoid processes by an osseous ring, the caroticoclinoidal ring.

Posteriorly, the sella turcica is bordered by the dorsum sellae (Fig. 2.3a) and the posterior clinoid processes (Fig. 2.3a). Anterior and caudal to the dorsum sellae, venous lacunae are found between the periosteal linings and the pituitary capsule [13], including the posterior intercavernous sinus and basilar sinus [14]. Connections between the posterior intercavernous sinus and the anterior intercavernous sinus

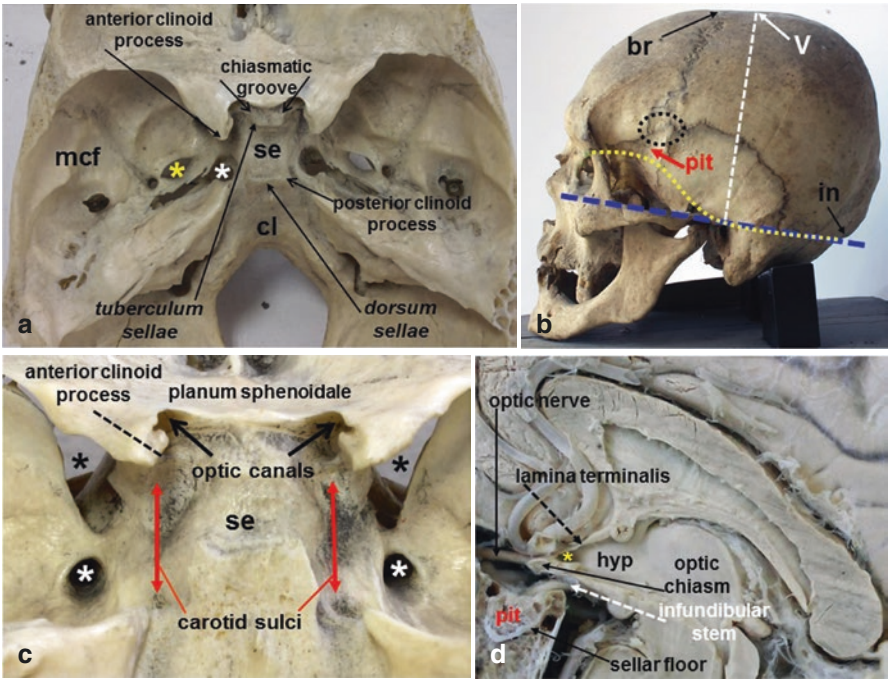

Fig. 2.3 (**a**) Middle cranial fossa (mcf) of an adult human skull showing the location of the sella turcica (se), a saddle-shaped groove in the superior part of the sphenoid in continuity with the dorsum sellae and clivus (cl) of the occipital bone. A number of other bony landmarks relevant to the anatomy of the sellar region are shown; white asterisk, the foramen lacerum allowing the passage of the internal carotid artery; yellow asterisk, the foramen ovale allowing the passage of the mandibular branch of the trigeminal nerve. (**b**) Lateral projection of an adult human skull. The location of the sellar region and pituitary gland (pit) are indicated by the red arrow, just inferior to the pterion (black dotted circle), the area of intersection between the sphenotemporal, sphenoparietal, and sphenofrontal sutures. The pituitary lies some centimeters anterior to the intersection of Frankfurt plane (blue dotted line) and the line connecting the vertex of the cranial vault (V) with the external acoustic meatus. Due to the sinusoidal shape of the cranial base profile (yellow dotted line), however, the pituitary fossa is pushed upward toward the center of the temple; *br* bregma, *in* inion or external occipital protuberance. (**c**) Optic canals (black arrows) allow the passage of the optic nerves and ophthalmic artery and are located anterior to the sella (se) and medially to the superior orbital fissure (black asterisk), where the oculomotor, trochlear, abducens, and ophthalmic branch of the trigeminal nerves and ophthalmic veins course. Below is the foramen rotundum (white asterisk) allowing entry of the maxillary branch of the trigeminal nerve. The internal carotid artery courses laterally and inferiorly to the sella in the carotid sulci (red arrows). (**d**) Sagittal section of an adult, human brain showing the major, neuroanatomical structures lying above the sella turcica and pituitary gland. *pit* pituitary, *hyp* hypothalamus, yellow asterisk = optic recess of the third ventricle. (All images (**a**–**d**) courtesy of the Museum of Biomedicine – BIOMED, University of Parma, Parma, Italy)

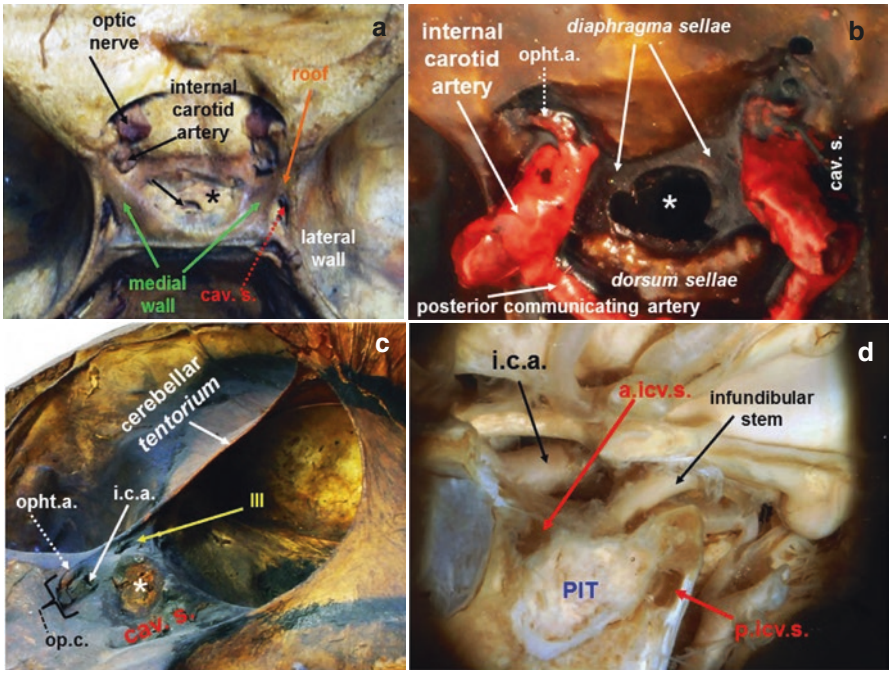

Fig. 2.4 (**a**, **b**) Views from behind and above the human sella turcica (dehydrated preparations); (**a**) Adult subject, (**b**) infant. (**a**) The sella is covered by a meningeal lining (asterisk) and contains a central opening (arrow) through which the pituitary stalk enters the pituitary fossa. The medial walls and roof of the cavernous sinus (cav.s.) circumscribe the pituitary. (**b**) The course of the horizontal segment of the internal carotid artery within the cavernous sinus (cav.s.) and emergence of the ophthalmic artery (opht. a.) is well delineated following injection with colored resin. Note dark, meningeal lining of the roof continuous with the diaphragma sellae. Central opening of diaphragma is denoted by an asterisk. (**c**) View from above and left side of the endocranial surface of the human cranial base (dehydrated preparation, adult subject). The central opening in the diaphragma sellae reveals the underlying pituitary tissue (asterisk). The oculomotor nerve (III) courses within the lateral wall of the cavernous sinus (cav.s.), and the ophthalmic artery (opht.a.) is seen arising from the internal carotid artery (i.c.a.) and to enter the optic canal (op.c.). The meningeal lining of the diaphragma is continuous with the free edge of the meningeal cerebellar tentorium that is fused with the lateral wall of the cavernous sinus. (**d**) Detail of a sagittal section of an adult, human brain. The internal carotid artery (i.c.a.) courses lateral to the pituitary gland (PIT) and surrounded anteriorly and posteriorly by the anterior intercavernous sinus (a.icv.s) and posterior intercavernous sinus (p.icv.s.), respectively. (All images courtesy of the Museum of Biomedicine – BIOMED, University of Parma, Pama, Italy)

(Fig. 2.4d), which run along the anterior wall of the sella, contribute to a ring of venous lacunae around the pituitary called the circular sinus. The basilar sinus collects blood from the superior and inferior petrosal sinuses and is the most consistent, intercavernous connection across the midline [14].

Superiorly, the inner meningeal layer forms the roof of the cavernous sinus (Fig. 2.4a) and expands medially to form the roof of the sella turcica (Fig. 2.4a, b),

called the diaphragma sellae [15]. It is located ~5–10mm below the optic chiasm [16] and, in most instances, extends from the tuberculum sellae to the dorsum sellae measuring 11–13 × 8–10 mm (w × l) to cover the pituitary gland [17]. It has a central, circular opening of ~5 mm to allow the passage of the pituitary stalk (Fig. 2.4a, b). At the level of this orifice, the inner meningeal layer and leptomeninges (arachnoid and pia mater) of the suprasellar arachnoid cisternae (suprachiasmatic, interpeduncular, and lamina terminalis) and base of the brain fuse with the capsule of the pituitary gland [13], preventing the development of subdural and infra-arachnoid spaces within the pituitary fossa. However, in ~50% of normal subjects, an outpouching of arachnoid protrudes into the sella through the central opening and can give rise to an empty sella (see section "Radiologic Anatomy") or, if resected, predispose to the development of a cerebrospinal leak following transsphenoidal surgery [18].

Inferiorly, the floor of the sella turcica is made up of a thin layer of the bone covered by outer periosteal dura, sometimes containing an inferior intercavernous sinus similar to that described above pertaining to the sinuses in the posterior and anterior sellar walls. The sellar floor separates the pituitary fossa from a pneumatic cavity within the body of the sphenoid bone, the sphenoid sinus. This sinus has an average depth of ~2 cm [14] and communicates with the nasal space (Fig. 2.5a) through an ostium that opens superiorly and behind the superior nasal conchae of the ethmoid, corresponding to the sphenoethmoidal recess (Fig. 2.5b). Rarely, the sellar floor connects the pituitary fossa with the posterior part of the nasopharynx through a craniopharyngeal canal, terminating ~1.5 mm behind the posterosuperior angle of the nasal vomer [19–21]. The craniopharyngeal canal, a remnant of the migration pathway taken by the embryonic pituitary to reach the sella turcica (see section "Embryologic Anatomy") and lined by dura mater, may persist in the adults and contain functional pituitary tissue [19].

The sphenoid sinus serves as the primary, anatomical landmark for the transsphenoidal approach to the sella turcica. In ~75% of adults, the sphenoid sinus is entirely pneumatized and located below the floor of the sella turcica, even extending up to the clivus (sellar type) (Fig. 2.5a, b). Otherwise, it terminates at the level of the anterior sellar wall (presellar type) (Fig. 2.5c). In both instances, the sellar floor thickness ranges from 0.1 to 1.5 mm. In young children, however, a pneumatized sphenoid is lacking, and the floor of the sella can be up to 10 mm thick. Most often (~70% of adults), the sphenoid sinus is asymmetrically divided into two, separate spaces by a bony septum (intersphenoid septum) but can contain multiple smaller septa to further loculate each space [14]. The internal carotid artery courses along and external to the lateral walls of the sphenoid sinus, giving rise to a carotid prominence inside the sinus.

Craniometric parameters used to identify and/or predict changes in the macroscopic morphology of the pituitary gland include the sellar length and width. The sellar length is greatest in the anterior-posterior diameter of the pituitary fossa when measured at the level of the tuberculum sellae or below, whereas the sellar width is defined as the distance between the two carotid sulci at the level of the sellar floor (Fig. 2.3c). In most Caucasian adults, the upper limit of normal is 17 × 15 mm [14]. The depth of the sella generally does not exceed 13 mm when the greatest distance between the sellar floor and a perpendicular line connecting the tuberculum and dorsum is measured [14].

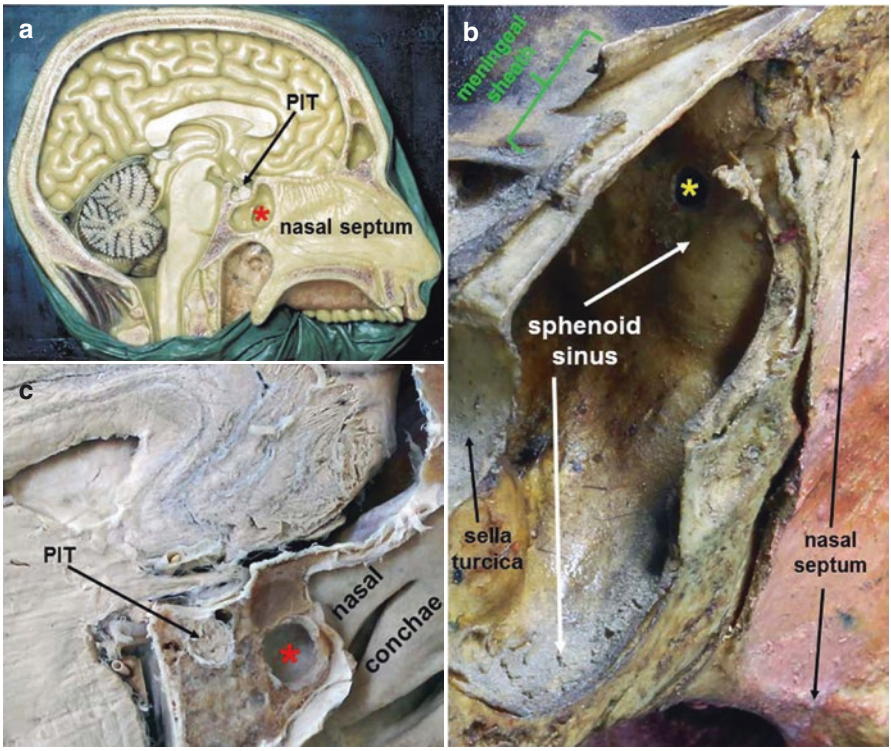

Fig. 2.5 (**a**) Sagittal section of the human head and brain. The sphenoid sinus (sellar type, red asterisk) lies in front of and beneath the sella turcica harboring the pituitary gland (PIT) (nineteenth-century anatomical wax preparation by Cesare Bettini, courtesy of the Collection of Anatomical Waxes "Luigi Cattaneo," University of Bologna, Bologna, Italy). (**b**) Detail and enlargement of a sagittal section of the adult, human sphenoid sinus (dehydrated specimen of the skull and meninges). The sinus opens into the sphenoethmoidal recess through an ostium (yellow asterisk) and communicates with the endonasal space. (**c**) Sagittal section of an adult, human brain showing the sphenoid sinus (presellar type, red asterisk) and its relationship to the pituitary gland (PIT) and nasal conchae. ((**b**, **c**) Courtesy of the Museum of Biomedicine – BIOMED, University of Parma, Parma, Italy)

Pituitary Gland

The pituitary gland is composed of an anterior, epithelial lobe (anterior pituitary or adenohypophysis) and a posterior neural lobe (neurohypophysis) (Fig. 2.6a). In man, the wet weight of the entire gland is proportional to its volume. It increases from ~100 mg at birth to ~500–600mg during the second decade depending upon ethnicity [22, 23] and may even reach 800 mg in males and 900 mg in females [24]. Women generally have a pituitary that is ~20% larger than men [22] and can double its weight during pregnancy and with a progressive increase in multiparity [24]. These changes are confined to the anterior lobe, however, as the size and weight of the posterior lobe remain fairly constant throughout life [22, 25] and it does not display sexual dimorphism [26]. In general, the adult hypophysis measures approximately 10 mm in length, 10–15 mm in width, and 5 mm in height [22].

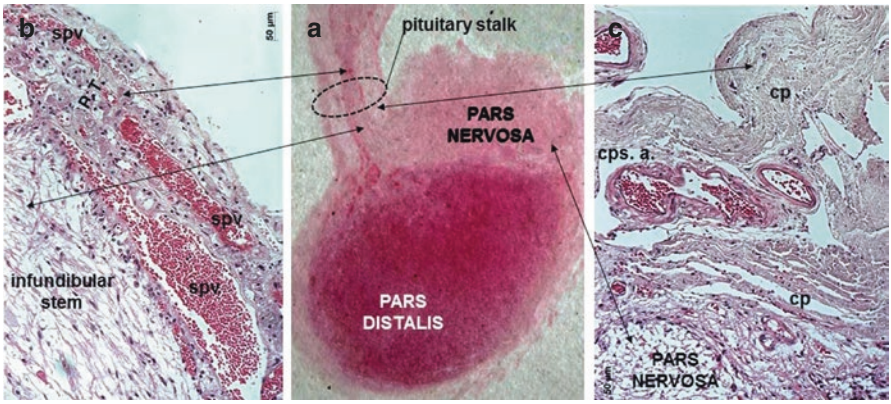

Fig. 2.6 (**a**) Sagittal section (hematoxylin and eosin staining) of the human pituitary gland and pituitary stalk (Courtesy of Cristina Micheloni, Section of Human Anatomy – DIMEC, University of Parma, Parma, Italy). (**b**) The pituitary stalk is shown under higher magnification. The pars tuberalis (P.T.) covers neural tissue of the infundibular stem and contains numerous short portal vessels (spv). (**c**) The posterior pituitary or pars nervosa and infundibular stem are enveloped by a fibrous capsule (cp) enriched by branches of the capsular artery (cps.a.) arising from the inferior hypophysial artery

The entire gland is surrounded by a fibrous capsule organized into two layers (Fig. 2.6c). The first is an inner layer of lamina propria made up of collagen types 1–5 [27] that gives rise to fibrous trabeculae that penetrate the adenohypophysial parenchyma [13] and segments it into three, main territories, a central mucoid wedge (named because of its strong PAS positivity, otherwise known as the pars interloralis, see Figs. 2.15a, e and 2.17b) and two lateral wings [28]. These fibrous trabeculae (called the fibrous core) provide passage for arterial branches that perfuse adenohypophysial parenchyma [29] and described further below. The second is a thicker, external layer made up of collagen types 1, 2, and 4 [13] that forms the lateral walls and roof of the sella [27, 30]. The external layer is a periphypophysial extension of the dural sheath and presumed to be the true pituitary capsule [13]. Since the capsule is loosely attached to the lamina propria through connective fibers that fills a potential space between them, the anterior lobe retains some degree of passive movement, as observed in cases of adenohypophysial displacement to one side of the sella in the presence of an enlarging pituitary adenoma [13]. In contrast, at the level of the neurohypophysis, the two adenohypophysial capsular layers fuse to each other, preventing movement of the posterior pituitary [13].

The anterior lobe contains three subdivisions including the pars distalis, pars intermedia, and pars tuberalis. The pars distalis lies adjacent to the pars nervosa but demarcated by an epithelial lamina corresponding to the pars intermedia. Rarely, the pars distalis envelops the pars nervosa or is detached from it, resulting in protrusion of the neurohypophysis into a depression of the dorsum sellae [24]. The pars distalis makes up the bulk of the anterior pituitary and contains all of the hormone-secreting cells of the adenohypophysis (see section "Microscopic Anatomy"). The pars intermedia lies between the pars distalis and the posterior pituitary, representing what

remains of the posterior loop of Rathke's pouch (see section "Embryologic Anatomy"). The pars tuberalis can be subdivided into a superior part attached to the hypothalamic median eminence, and an inferior part that surrounds the infundibular stem (Fig. 2.6b) but separated from it by a fibrovascular lamina (septum tuberalis) that contains the portal vessels [29, 31].

The neurohypophysis is comprised of the posterior pituitary and infundibular stem (the neural component of the pituitary stalk, the latter also including the pars tuberalis) that extends from the floor of the hypothalamus (a protrusion of the hypothalamic tuber cinereum that contains the infundibular recess of the third ventricle) to the posterior pituitary. Where the infundibular stem joins the posterior pituitary, the pars distalis forms two, symmetric groves called the loral groves, into which the loral arteries pass to enter the pars distalis (see section "Vascularization of the Pituitary Gland"). The lower part of the stem forms a genu that displaces adenohypophysial tissue anteriorly and is covered by a continuation of the septum tuberalis (described above) called the genual septum. It is through the genual septum that the portal vessels as well as other pituitary arteries pass into the pars distalis (see section "Vascularization of the Pituitary Gland").

Pituitary tissue can also be present in the nasopharynx, commonly referred to as a pharyngeal pituitary [32]. This structure is a residual of Rathke's pouch during its migration from the oral cavity to the middle cranial fossa (see section "Embryologic Anatomy") and situated in the mucoperiosteum between the sphenoid and vomer bones [33]. Typically, it is observed as a compact, elongated cell group 2–5 × 0.2–0.5 mm (l × w) that contains an incomplete fibrous capsule and occupies a volume ranging from 0.13% to 0.5% of the normal pituitary [34, 35]. All cell types in the pars distalis are also present in the pharyngeal pituitary [34, 36], and because of its connections with the sellar hypophysis via transsphenoidal venous and arterial vessels originating from the vomerosphenoidal fossa, sellar intercavernous sinus, sellar arteries, and possibly stalk portal vessels [37, 38], it can be functional [39].

Vascularization of the Pituitary Gland

The human pituitary gland is a highly vascular structure that receives both direct (arterial) and indirect (sinusoidal) vascularization. Direct vascularization originates from the supracavernous portion of the internal carotid arteries that give rise to lateral and anterior superior hypophysial arteries and the intercavernous portion of the internal carotid artery that gives rise to the inferior hypophysial arteries. The lateral and anterior superior hypophysial arteries give off numerous short branches that course along the long axis of the infundibular stem and terminate in capillary complexes at its upper part. The superior hypophysial artery also gives rise to the loral artery (also known as the middle hypophysial artery or artery of the trabecula) [40, 41]. It enters the superior surface of the anterior lobe at the homolateral loral groove to perfuse the region between the mucoid wedge and the lateral wings of the pars distalis and gives off branches that extend upward onto the surface of the pars

tuberalis to anastomose with long branches of the anterior superior hypophysial artery [40], contributing to the vascularization of the pituitary stalk and a small part of the posterior pituitary [29]. Collectively, therefore, the superior hypophysial artery serves both the stalk and anterior lobe [42].

The inferior hypophysial artery on either side of the pituitary divides into ascending and descending branches running in the groove between the anterior and posterior pituitary lobes and anastomoses with each other, giving rise to an arterial circle that penetrates the posterior lobe or courses along the capsular surface of the neurohypophysis (Fig. 2.6c) to perfuse this tissue [29, 40]. Some vessels also extend over the inferior surface of the pars distalis to penetrate adenohypophysial parenchyma [29]. Collectively, this arrangement indicates that the inferior hypophysial artery primarily serves the posterior lobe and, to a minor extent, the adenohypophysis [42].

The most critical source of the vascularization to the anterior pituitary, however, is the pituitary portal system, originally identified as "portal veins" because its vessels act as a link between the arterial blood of the hypophysial arteries and venous blood of the hypophysial veins [43]. However, technically, the human hypophysial-portal veins are really fenestrated sinusoids originating from the surface of the hypothalamic median eminence and infundibulum [29]. They remain superficial and collect a network of deeper sinusoidal capillaries stemming from the branches of the superior and inferior hypophysial arteries that form capillary tufts (so-called gomitoli) within the neural tissue of the hypothalamic infundibulum, infundibular stem, and neurohypophysial genu [29]. The portal sinusoids include a posterior and anterior group. The posterior group gives rise to the long portal vessels that enter the bulk of the pars distalis, whereas the anterior group is the source of the short portal vessels that form in a region of the infundibular stem beneath the pars tuberalis (septum tuberalis) (Fig. 2.6b) and neurohypophysial genu and terminate in the mucoid wedge and lateral wings of the pars distalis [29].

The venous drainage from the pituitary gland is primarily directed into the cavernous sinuses, although some venous blood also drains into the circular sinus and the inferior sinus. Portal sinusoids within the adenohypophysis join together to form small, collecting channels (the lateral and anteroinferior hypophysial veins) located lateral to the gland before emptying into one of its venous perihypophysial sinuses [40, 44]. Other veins are formed in the superior part of the pars distalis (superior hypophysial veins) and drain into a venous plexus at its dorsal surface. Ultimately, the pituitary blood drains from the cavernous sinuses into the superior and inferior petrosal sinuses. Some authors have also observed drainage from hypophysial stalk sinusoids into the sellar circular sinus [44] and the venous network of the pia mater [40], but this is only minor. Venous efferents from the posterior pituitary run parallel to the inferior hypophysial artery and mainly drain into the posterior hypophysial sinus and a plexus of veins lying posterior to the posterior pituitary (posterior venous network) that drain both the intercavernous/cavernous sinuses and cranial basilar sinus [44].

Embryologic Anatomy

In man, the anterior pituitary derives from a specialization of the embryonic ectoderm bordering the most anterior and ventral portion of the neural tube [45] that in the early, vertebrate embryo corresponds to the preplacodal ectoderm of the neural plate [46]. At the beginning of the 4th week of fetal development, the neural tube closes, but a cranial opening remains, the anterior neuropore, that quickly collapses to become the anterior wall of the proencephalic vesicle. Below the anterior neuropore is the frontotemporal ectoderm of the neural tube that adjoins with the mouth opening or stomodeum inferiorly. At the level of the most ventral and median part of the frontotemporal ectoderm, fusion occurs with ectodermal cells of the surface epithelium (the epidermis), enveloping the entire neural tube and body of the embryo [45]. This "mixed" ectodermal structure (neural tube ectoderm/surface ectoderm) invaginates backward into the stomodeum to line its roof but, at this stage, is not separated from the overlying neural tube by the mesoderm. Only later, the mesoderm interposes to form the sphenoid bone (see below), moving anteriorly from the notochord and terminating behind a temporary closure of the stomodeum, the fenestrated buccopharyngeal membrane. As a result, a "specialized" ectoderm develops anterior to the buccopharyngeal membrane, the adenohypophysial placode, the source of tissue lining the roof of the oral aperture. Whether in man, the adjacent neural crest forming the thickened "lips" of the anterior neuropore contributes to the adenohypophysial placode is not known. By analogy with other vertebrates, however, it is assumed that the preplacodal ectoderm is devoid of neural crest cells [46]. However, it is suggested that the adenohypophysial placode might contain neural crest cells [47], and recent immunocytochemical data in human embryos support this possibility [48, 49].

Around the 4th to 5th weeks of fetal development, the adenohypophysial placode emits a dorsally directed evagination, Rathke's diverticulum, that moves upward throughout the mesoderm that is now interposed between the roof of the buccal cavity and the ventral surface of the proencephalon [50]. This mesoderm, called the prechordal ectomesenchyme (because it is positioned anterior to the notochord), contains neural crest cells arising from the mesencephalic crest [51]. Rathke's diverticulum elongates inside the prechordal ectomesenchyme, forming a pharyngohypophysial stalk that will come in contact with the floor of the diencephalic vesicle which will become the hypothalamic infundibulum. At the same time, the future superior hypophysial artery develops from the ectomesenchyme below the diencephalic vesicle, giving off branches to the primordium of the hypothalamic infundibulum [52]. Around the 6th to 7th weeks of fetal development, the floor of the diencephalic vesicle extrudes a neural diverticulum, the primordium of the infundibular stem, that moves inferiorly toward the tip and posterior surface of Rathke's diverticulum, the latter progressively closing to form a pouch or Rathke's pouch that loses continuity with the oral cavity (Fig. 2.7a). At this stage, the placodal cells of the tip of Rathke's pouch wrap around the primordial infundibular stem to eventu-

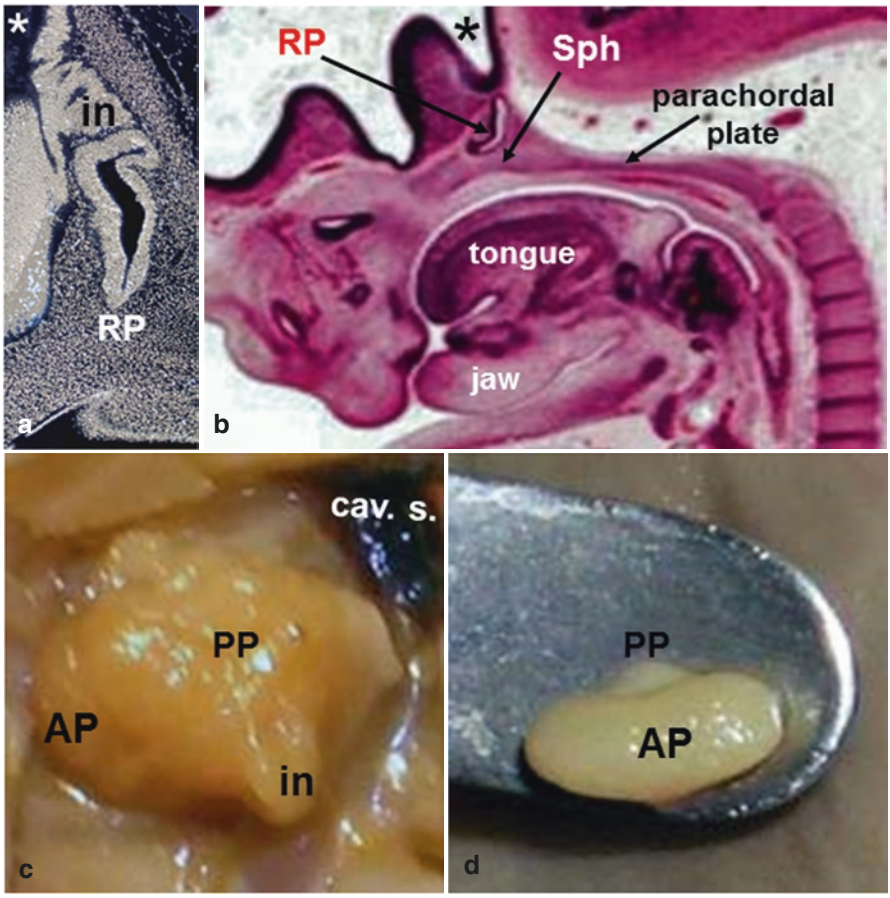

Fig. 2.7 (**a**, **b**) Midsagittal sections of two, human embryos at 6 and 7 fetal weeks, respectively (H&E staining, magnification × 10). (**a**) Rathke's pouch (RP) has just closed and joins with the tip of the primordial infundibular stem (in) extruding from the floor of the third ventricle (asterisk). (**b**) The base of Rathke's pouch is now separated from the buccal floor and located in the primordial sella turcica of the sphenoid bone (Sph) developing in the ectomesenchyme cranial to the parachordal plate of the notochord. Asterisk = third ventricle. (**c**, **d**) Macroscopic dissection of two human fetuses at 17 and 21 fetal weeks, respectively. (**c**) The pituitary gland is in the sella turcica and tilted forward. The posterior pituitary (PP) is well demarcated from the anterior pituitary (AP) and continuous with the infundibular stem (in). Laterally, the right cavernous sinus (cav.s.) is visible. (**d**) The pituitary gland has been removed from the sella turcica. The bulk of the anterior pituitary (AP) is already well formed, and the pars distalis is enlarging laterally, anterior to the posterior pituitary (PP)

ally become the adenohypophysial pars tuberalis (see below) [50]. Rathke's pouch separates from the stomodeal roof due to the development of cartilage of the primordial sphenoid bone (Fig. 2.7b). Only a mesenchyme-filled channel through the sphenoidal cartilage remains, the craniopharyngeal canal, that will later involute, although occasionally remains as a part of a developmental disorder [19]. During

the 8th week of fetal development, sinusoidal connections with the superior hypophysial artery appear in the prechordal ectomesenchyme, invading Rathke's pouch to become the intrapituitary fibrous septa and giving rise the primordial hypophysial-portal vessels that will later proliferate within the pars distalis [52]. During this developmental period, the prechordal ectomesenchyme also proliferates anteriorly and inferiorly to give rise to the so-called nasal trabecula (i.e., the primordium of the nasal septum) [53]. Thus, the cartilage of the nasal septum contains neural crest cells and of the same type believed to contribute to the development of the human pituitary [48, 49].

The ectomesenchymal area of the nasopharynx, at the interphase between the inferior surface of the developing sphenoid and the vomer bones, encases the posterior aspect of the nasal septum where the buccopharyngeal membrane ceases and Rathke's pouch arises in the oral cavity. At this location, between the 8th and 10th weeks of fetal development, an ectodermal pituitary outgrowth, the buccohypophysial stalk, segregates between the external layer of ectomesenchyme (later forming the periosteum of the sphenoid) and the epithelial lining of the pharynx to become the pharyngeal pituitary. By the end of the first trimester of pregnancy, the pharyngeal pituitary is highly vascularized by branches of pharyngeal arteries and by venous conduits originating from intracranial venous sinuses in the region of the future sella turcica and exhibits signs of eosinophilic and basophilic histodifferentiation. However, numerous cells display cytological features of undifferentiated elements [54–56].

The prechordal ectomesenchyme of the sphenoid bone is also believed to be critical for the specification of different adenohypophysial cell types from placodal cells. Between the 8th and 9th weeks of fetal development, Rathke's pouch forms three diverticula, a single median, and two laterals. The upper part of the lateral diverticula gives rise to the pars tuberalis, whereas the median diverticulum provides the epithelial bulk of the mucoid wedge in the fully differentiated gland. Simultaneously, the first corticotrophs and thyrotrophs differentiate in the lower diverticular parts in direct contact with the surrounding ectomesenchyme [50]. During the 13th week of fetal development, somatotrophs and gonadotrophs differentiate in the lower portions of the lateral diverticulum of Rathke's pouch, increasing in number throughout the 21st–29th weeks. At these developmental stages, the neural lobe acquires a well-defined morphology (Fig. 2.7c), and the bulk of the corticotrophs differentiate in the walls of the median diverticulum, including that in contact with the primordial infundibular stem, the pars intermedia. Concurrently, thyrotrophs and gonadotrophs become detectable in the pars tuberalis. Since anencephalic fetuses lack corticotrophs and gonadotrophs, it has been suggested that early contact with the primordial neurohypophysial tissue may have a key role for the histodifferentiation of these two pituitary cell types in man [57]. Finally, starting in the 21st week of fetal development, lactotrophs are identified throughout the primordial pars distalis (Fig. 2.7d) that includes all three diverticula of Rathke's pouch [50].

During the last trimester, pituitary tissue completely surrounds the infundibular stem, and the primordial pars distalis enlarges laterally to give rise to the lateral wings,

Table 2.2 Transcription factors associated with genetic causes for human disorders of pituitary development and secretion

Transcription factor	Anterior pituitary deficiencies	Pituitary appearance by MRI
ARNT2	TSH, ACTH, variable GH, LH, FSH	Hypoplastic anterior pituitary, posterior pituitary can be absent
GLI2	Variable GH, PRL, TSH, LH, FSH, ACTH	Hypoplastic anterior pituitary, posterior pituitary can be ectopic or absent
HESX1	GH, variable PRL, TSH, LH, FSH, ACTH	Nl, hypoplastic or aplastic anterior pituitary, posterior pituitary can be ectopic
LHX3	GH, PRL, TSH, LH, FSH	Nl, hypoplastic or enlarged anterior pituitary
LHX4	GH, TSH, LH, FSH, variable ACTH	Hypoplastic anterior pituitary
OTX2	Variable GH, PRL, TSH, LH, FSH, ACTH	Nl, hypoplastic or ectopic anterior pituitary, posterior pituitary can be ectopic
PAX6	Variable GH, TSH, LH, FSH, ACTH	Nl or hypoplastic anterior pituitary
POU1F1 (PIT-1)	GH, PRL, variable TSH	Nl or hypoplastic anterior pituitary
PROP1[a]	GH, PRL, TSH, variable LH, FSH and ACTH	Nl, hypoplastic or enlarged anterior pituitary
SOX 2/SOX 3	Variable GH, TSH, LH, FSH, ACTH	Hypoplastic or enlarged anterior pituitary, posterior pituitary can be ectopic
TPIT (TBX19)	ACTH	Nl anterior pituitary

Adapted from Di Iorgi et al. [159], Giordano [160], and McCabe and Dattani [62]
[a]Most common genetic cause for combined pituitary hormone deficiency

as in the adult (Fig. 2.7c). Although the cavity of Rathke's pouch is still present, follicular structures are progressively formed in its vicinity as a part of protrusions from its walls, the posterior one becoming the pars intermedia. Due to the strong morphological similarity between folliculostellate cells and the free surface epithelium of Rathke's cavity, it is presumed that the cells that make up the follicular structures are precursors of the human folliculostellate cells [50]. Numerous genes and transcription factors are involved in regulating the various developmental steps of the human pituitary and are extensively reviewed elsewhere [58–63]. A summary of transcription factors relevant to human, pituitary morphogenesis, and histodifferentiation is provided in Table 2.2, based on clinical outcomes when any of these factors are mutated. A schematic summary of the sequential actions of transcription and other morphogenetic factors to induce the different adenohypophysial cell types is shown in Fig. 2.8.

Radiologic Anatomy

The introduction of computed tomography (CT) and magnetic resonance imaging (MRI) into medical practice has provided highly sensitive tools to elucidate the normal anatomy of the pituitary gland and to identify pathology. In particular, by MRI, the anterior and posterior pituitary are well delineated in T1-weighted images by the

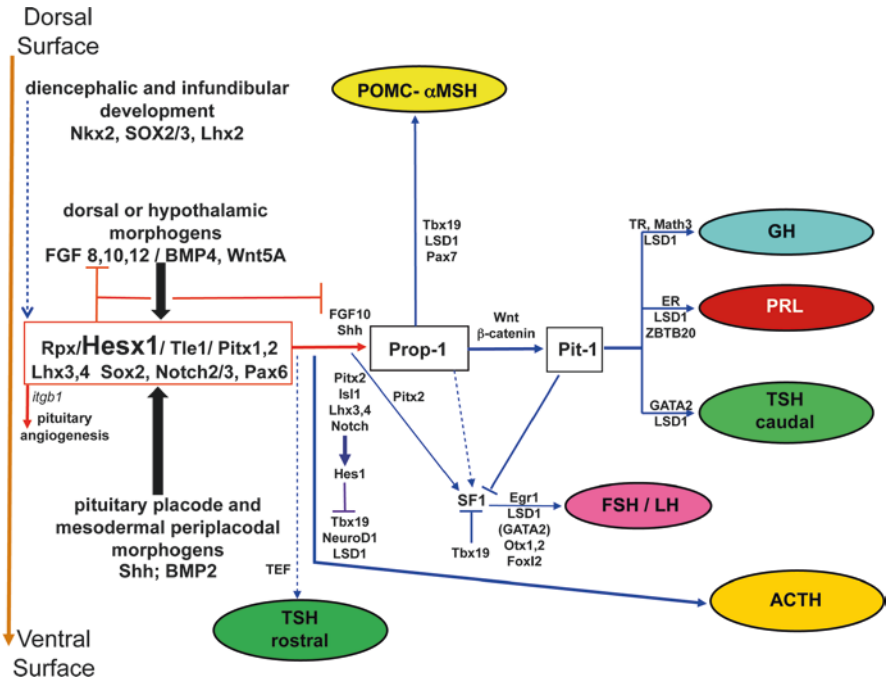

Fig. 2.8 Signaling molecules and transcription factors involved in the development of the anterior pituitary, including its vascularization (based on rodent studies). Anterior lobe somatotrophs, lactotrophs, and caudally placed thyrotrophs derive from a common lineage, determined by Prop-1 and Pit-1. Independent lineages are observed for a rostrally placed group of thyrotrophs, corticotrophs, gonadotrophs, and intermediate lobe melanotrophs. All cell types are committed to a specific lineage through activation of Notch signaling at the placodal stage. Development of the entire pituitary anlagen and related cell types are also dependent on interactions with the diencephalon and infundibular stem, whose morphogenesis is under particular influence by Hesx1. Continuous arrows, direct stimulatory action; dotted arrows, indirect stimulatory action; blocked line, inhibitory action. (Modified from Lechan and Toni [5])

so-called bright spot of the posterior pituitary (Fig. 2.9a), the posterior pituitary being hyperintense relative to gray matter despite the absence of contrast [64]. The bright spot is observed in up to 100% of normal adults, although can be absent in older individuals, possibly due to reduced storage of neurosecretory material. Typically, the bright spot measures between 1.2 and 8.5 mm in its greatest diameter and between 0.4 and 4.4 mm in the axis perpendicular to the longest axis [64]. Anything larger should raise suspicion of the underlying pathology such as a Rathke's cleft cyst (Fig. 2.9b) or hemorrhagic pituitary adenoma. It has been proposed that the bright spot can be a useful diagnostic tool to differentiate central diabetes insipidus from psychogenic polydipsia, as in central diabetes insipidus, the bright spot is absent [65] (Fig. 2.9c), whereas in psychogenic polydipsia, the bright spot is present, perhaps even larger than normal due to increased accumulation of neurosecretory material [66, 67]. The posterior pituitary has tremendous regenerative capacity such

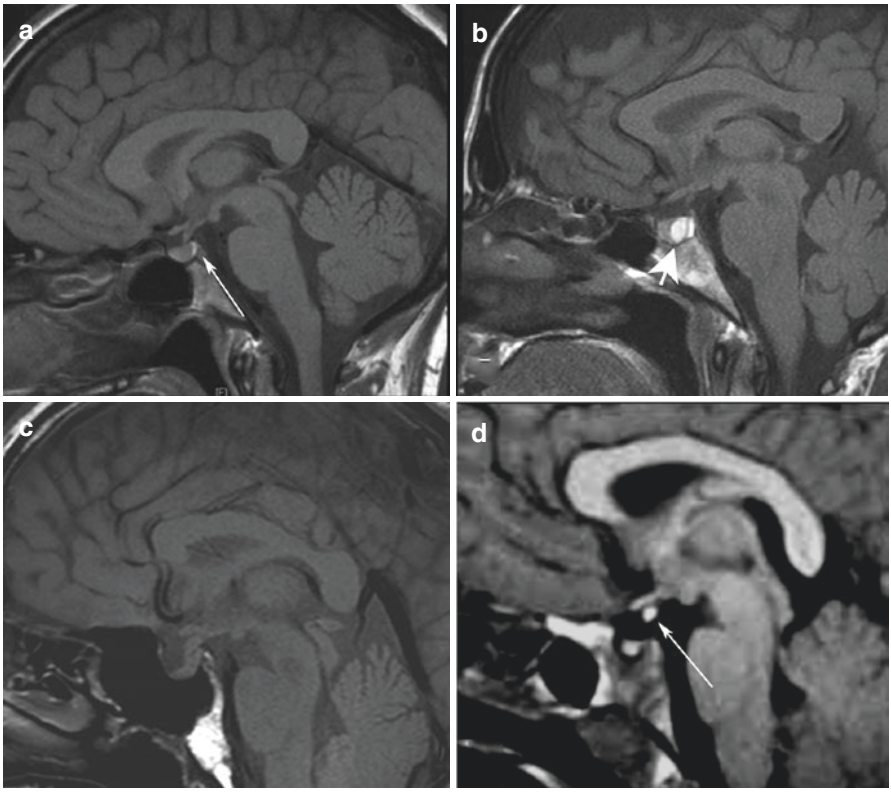

Fig. 2.9 Sagittal views of the adult, human brain by MRI. (**a**) Normal radiologic anatomy of the pituitary gland in a T1-weighted image. Note the flat to slightly concave upper surface of the pituitary and the typical appearance of the "bright spot" (arrow) denoting the posterior pituitary. The pituitary stalk is directed anteriorly and tapers as it enters the pituitary gland, the diameter of the proximal portion being somewhat larger due to invagination of the third ventricle to create the infundibular recess. (**b**) Bright spot of the posterior pituitary should not be confused with pathology such as Rathke's cleft cyst (arrowhead) which can also appear hyperintense on T1-weighted images. (**c**) Absent "bright spot" in a patient with diabetes insipidus secondary to neuroinfundibulitis. Note marked thickening of the pituitary stalk. (**c**) Ectopic posterior pituitary following stalk transection. Note the location of "bright spot" in the suprasellar cistern (arrow), absence of the pituitary stalk, and small size of the anterior pituitary

that with transection of the pituitary stalk, a new, functional posterior pituitary can form, apparent as a bright spot in an ectopic location, generally the suprasellar cistern (Fig. 2.9d).

The anterior pituitary is isointense to gray matter on T1-weighted images and isointense to hypointense on T2-weighted images and generally has a flat or concave superior surface (Fig. 2.9a). In keeping with the macroscopic anatomy (see above), the pituitary volume by MRI shows significant differences between the sexes and with aging [68–71]. In general, the anterior pituitary is small and flattened during most of childhood but enlarges during puberty, somewhat more in girls than

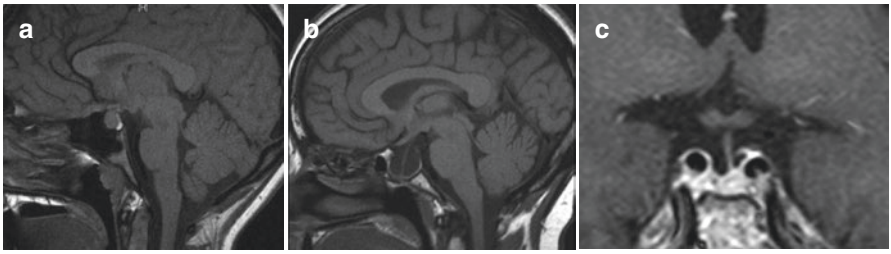

Fig. 2.10 (**a**, **b**) Sagittal and (**c**) coronal views of the adult, human brain by MRI showing normal variations of the pituitary and stalk. (**a**) Enlarged anterior pituitary in a normal, adolescent woman demonstrating convex superior surface extending into the suprasellar cistern. (**b**) Empty sella in an individual with otherwise normal anterior and posterior pituitary function. (**c**) Slight deviation of the stalk to the left in a man with an asymmetric intersphenoid septum

boys, and then decreases in size in the aged [72–74]. In a Croatian study of 199 adults (91 males and 108 females), the mean pituitary volume by MRI in young men (ages 20–29) was 539.2 mm^3 and in females 680 mm^3, whereas in the aged (ages 70–79), it was 450.4 mm^3 in males and 636.3 mm^3 in females [68]. Adolescent women may have a convex superior border to the pituitary gland suggesting anterior pituitary hyperplasia (Fig. 2.10a), but this can be a normal appearance. A similar enlargement of the anterior pituitary by MRI is characteristic of pregnancy due to the proliferation of lactotrophs [75, 76], increasing in volume by as much as 120% by the third trimester, and may extend into the suprasellar cistern. This phenomenon reflects the tremendous plasticity intrinsic to the function of the anterior pituitary, capable of responding to a changing hormonal milieu. Marked enlargement of the anterior pituitary can also be observed in severely hypothyroid individuals due to hyperplasia of anterior pituitary thyrotrophs and in Addison's disease due to corticotroph hyperplasia, fully reversible with replacement of the deficient hormones [77, 78]. Anterior pituitary volume has also been observed to increase in association with anxiety and depression [79], likely secondary to the activation of the hypothalamic-pituitary-adrenal axis.

Occasionally, the anterior pituitary can appear flattened to the base of the sella turcica, commonly described as an "empty sella" (Fig. 2.10b). While this appearance can be indicative of underlying pathology (e.g., a pituitary adenoma that has undergone apoplexy, end stages of anterior pituitary hypophysitis, intracranial hypertension) [80], it may also be a normal variant due to herniation of arachnoid and cerebrospinal fluid into the sella turcica through an incompetent diaphragma sellae (see above, Pituitary Anatomy). Small cystic structures less than 2–3 mm can be observed on occasion in the central portions of the pituitary due to remnants of Rathke's pouch but incidental findings and of no real clinical significance.

The pituitary stalk is well visualized on MRI as a midline structure arising from the base of the hypothalamus coursing through the suprasellar cistern to terminate in the posterior pituitary (Fig. 2.9a). The characteristic tapering of the stalk from superior to inferior is due to the infundibular recess of the hypothalamus that results in an invagination of cerebrospinal fluid into the proximal portion of the stalk as an

extension of the third ventricle. Using high-resolution MRI (3T MR) in 29 healthy volunteers ages 21–43, the stalk diameter at the level of the optic chiasm measured 3.25 ± 0.39 mm, whereas at the pituitary insertion, it was 2.32 ± 0.39 mm [81]. On T2-weighted images in the majority of normal subjects, the central portion of the stalk is hyperintense compared to cerebral white matter due to neurosecretory material en route to the posterior pituitary and surrounded by a peripheral rim of isointensity, thought to represent pars tuberalis. Although stalk deviation often suggests underlying pathology, minor deviation of the stalk can be seen normally, particularly if there is some sloping of the sellar floor due to an eccentric location of the intersphenoid septum [82] (Fig. 2.10c).

The vascular anatomy of the pituitary, namely, that the posterior pituitary receives an arterial supply and the anterior pituitary is primarily (although not exclusively, see above, Vascular Anatomy) fed by sinusoidal blood coming from the portal circulation, can be appreciated with dynamic imaging of the pituitary in which MRI sequences are captured simultaneously with the intravenous administration of gadolinium. As would be anticipated, initial sequences show enhancement of the posterior pituitary and base of the hypothalamus, followed by enhancement of the pituitary stalk and finally the anterior pituitary (Fig. 2.11a–c) [83].

Many of the landmarks around the pituitary gland described above can also be well visualized by MRI, including the optic chiasm and structures in the cavernous sinus. The optic chiasm lies above the pituitary gland and can be central (directly over the pituitary ~65% of cases as shown in Fig. 2.9a), prefixed (more anterior to the pituitary ~25%), or post-fixed (more posterior over the pituitary ~10%). It is separated from the pituitary by the suprasellar cistern, which appears as a pentagonal, cerebrospinal fluid-filled space on coronal images (Fig. 2.12). The cavernous sinuses are located immediately lateral to the pituitary gland and contain vascular and neuronal elements. Most prominent in the cavernous sinus is the internal carotid artery, which appears hypointense on T1-weighted images because of the blood flowing through it (Fig. 2.12a). Cranial nerves III, IV, V_1, and V_2 sometimes can be visualized as hypointense filling defects by MRI, particularly cranial nerve III as shown in Fig. 2.12a. Sympathetic fibers encircle the carotid arteries but are not well visualized.

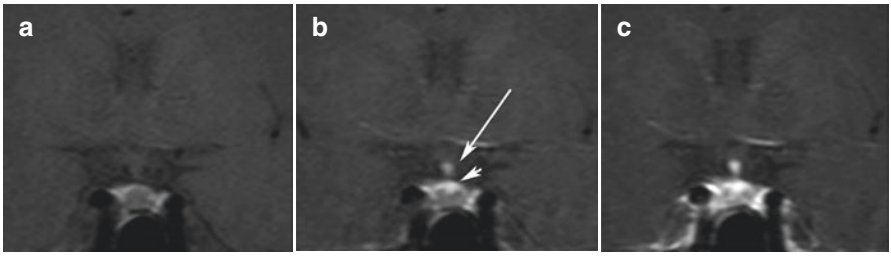

Fig. 2.11 Dynamic MRI in the coronal plane showing the time course of gadolinium filling of the pituitary following iv administration. (**a**) Pre-gadolinium. (**b**) Immediately post-gadolinium. The proximal pituitary stalk (arrow) and posterior pituitary (arrowhead) are the first to fill. (**c**) Gadolinium then fills the anterior pituitary

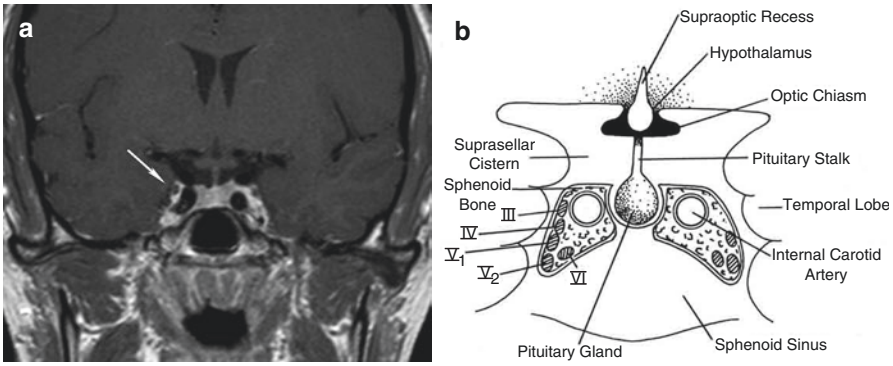

Fig. 2.12 (**a**) MRI and (**b**) schematic image of the pituitary and its anatomic relationships in coronal orientation. The cavernous sinus is situated on either side of the pituitary and contains the internal carotid artery and cranial nerves III, IV, V_1, V_2, and VI. The optic chiasm resides immediately above the pituitary gland and is separated from it by a pentagonal-shaped cerebrospinal fluid-filled space, the suprasellar cistern. Arrow in (**a**) points to cranial nerve III. (**b** from Endocrinol Metab Clin North Am, 16, Lechan RM, p 477, Copyright Elsevier)

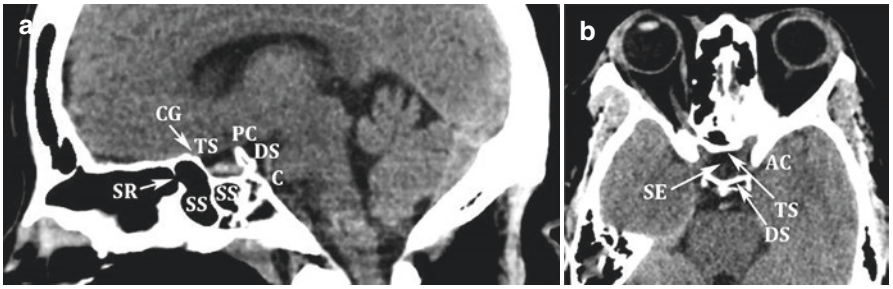

Fig. 2.13 (**a**) Parasagittal and (**b**) horizontal images of the sella turcica by CT. The bony architecture is well delineated. Note septations in the "sellar type" sphenoid sinus (SS). AC anterior clinoid, C clivus, CG chiasmatic groove, DS dorsum sellae, PC posterior clinoid, SE sella turcica, SR ostium of sphenoethmoidal recess, TS tuberculum sellae

MRI has largely replaced CT as the imaging modality of choice to assess the pituitary gland, but the bony architecture of the sella turcica is best seen by CT (Fig. 2.13). The clivus is also well seen as it slopes posteriorly and inferiorly from the dorsum sellae, as is the sphenoid sinus (Fig. 2.13). Mean length and height of the sella turcica by CT tend to be greater in females than in males [84], reflecting that the female gland is larger than the male gland.

Imaging using positron emission tomography (PET) is gaining increasing utility as newer tracers are being developed. ^{68}Ga-DOTATATE, which binds to somatostatin receptors 2 and 5, shows reasonably good uniform uptake throughout the normal, anterior pituitary due to its high expression of somatostatin receptors [85]. In contrast, 18F-FDG PET shows preferential uptake into pituitary adenomas as well

as other inflammatory and infiltrative disorders and little or no uptake into normal pituitary tissue [85], making it feasible to use PET imaging as a tool to identify tiny, functional pituitary adenomas by subtractive analysis.

Microscopic and Functional Anatomy

Anterior Pituitary (Adenohypophysis)

As noted above, the anterior pituitary is made up of three components, the pars distalis, the largest component of the anterior pituitary; pars intermedia, which is vestigial in man; and the pars tuberalis. It is the pars distalis, however, that is the main source of anterior pituitary hormone secretion.

Pars Distalis

The pars distalis is composed of nests or cords of large, epithelial, polygonal cells organized near venous sinusoids lined with a fenestrated epithelium into which secretory products from the anterior pituitary are collected. The nesting pattern is apparent in reticulin preparations that show a delicate, continuous border around acini (Fig. 2.14a), differentiating normal anterior pituitary tissue from adenomatous tissue that have a disrupted reticulin pattern (Fig. 2.14b). The cells of the normal pars distalis contain abundant cytoplasm that stain varyingly. Three cells types, acidophils, basophils, and chromophobes, were classically recognized using standard histological preparations such as hematoxylin and eosin (H&E) in which acidophils are red, basophils purple, and chromophobes light blue and PAS in which basophils are bright purple (Fig. 2.14c, d). A number of other stains have also been used in an attempt to identify specific cell subtypes, as illustrated in Fig. 2.14e, f, such as aldehyde thionine with PAS and orange G and Herlant stain. However, immunocytochemistry, which is now widely used in surgical pathology, best differentiates the five, major, cell types and six, secretory products of the anterior pituitary gland: somatotrophs (growth hormone), lactotrophs (prolactin), corticotrophs (adrenocorticotropic hormone), thyrotrophs (thyroid-stimulating hormone), and gonadotrophs (luteinizing hormone and follicle-stimulating hormone) (Table 2.3). The somatotrophs make up the acidophils (although lactotrophs can also be acidophilic), corticotrophs the basophils (although thyrotrophs can also be basophilic), and gonadotrophs, lactotrophs, and thyrotrophs the chromophobes. In fish, pituitary cell types tend to be highly organized into distinct zones, with lactotrophs more rostral and somatotrophs more caudal in the pars distalis [86]. A topography is also retained in man (Fig. 2.15) with a tendency for somatotrophs to occupy more lateral regions of the pars distalis, lactotrophs the posterolateral region, and corticotrophs

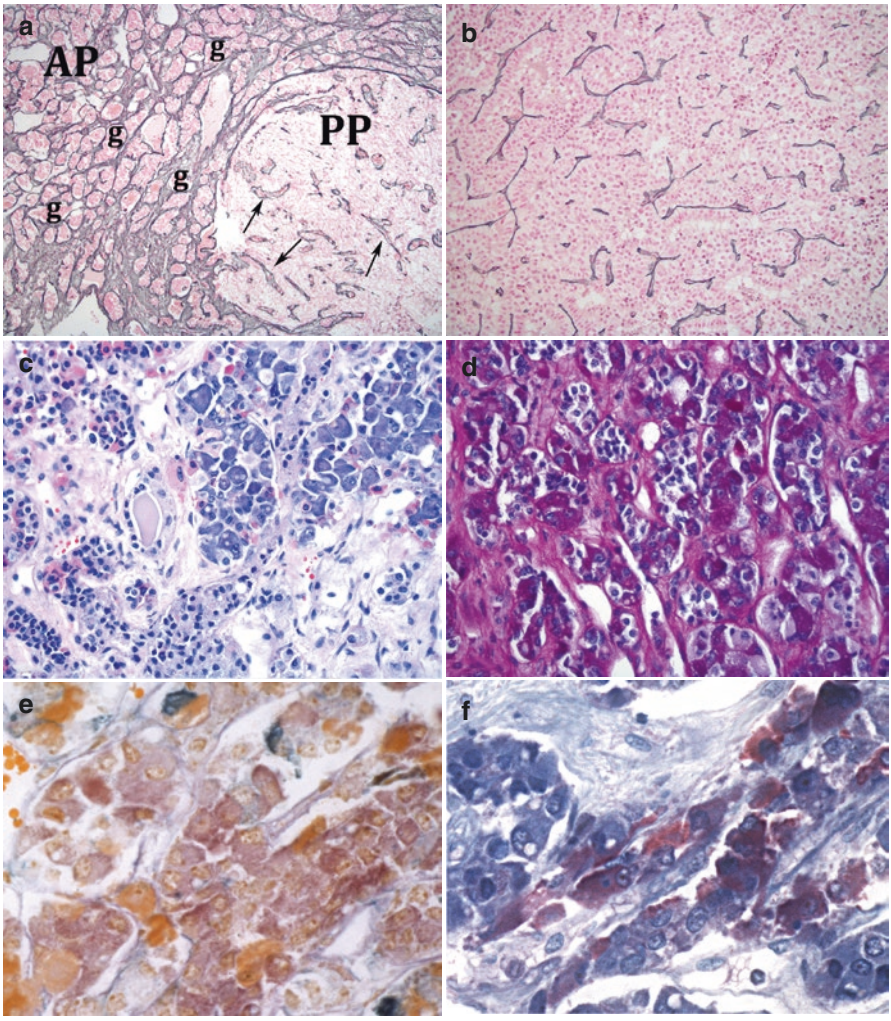

Fig. 2.14 Reticulin special stain of (**a**) normal pituitary and (**b**) pituitary adenoma. In the normal pituitary, reticulin fibers surround glandular (acini) components (g) of the pars distalis (PD) and decorate vessels (arrows) in the posterior pituitary (PP) but are discontinuous in pituitary adenomas with only capillaries picking up black staining. (**c**) H&E, (**d**) PAS, (**e**) PAS with aldehyde thionine orange G, and (**f**) Herlant stains of a normal pituitary. (**c**) Glands show mixed cell population including basophils (dark blue cytoplasm), acidophils (red cytoplasm), and chromophobes (light blue granular cytoplasm). Basophils show single or multiple small clear vacuoles in the cytoplasm, corresponding to enigmatic bodies. Yellow inclusions in some cells due to the presence of lipofuscin. (**d**) Only basophils avidly pick up PAS and appear bright purple. (**e**) Acidophils, which are largely somatotrophs, stain bright orange, gonadotrophs purple, and thyrotrophs dark blue. (**f**) Somatotrophs stain orange, lactotrophs red-purple, corticotrophs dark blue, and thyrotrophs light blue or unstained. Magnification ×200 in (**a**), ×400 in (**b**–**d**) and ×600 (**e**, **f**)

Table 2.3 Classic cell types and secretory products of the anterior pituitary

Cell type	Secretory products	% of cell population
Somatotroph	Growth hormone (GH)	50
Lactotroph	Prolactin	15
Corticotroph	Adrenocorticotropic hormone (ACTH)	15
Thyrotroph	Thyroid-stimulating hormone (TSH)	10
Gonadotroph	Luteinizing hormone (LH)	10
	Follicle-stimulating hormone (FSH)	

From *Endocrinol Metab Clin North Am*, 16, Lechan RM, p 477, Copyright Elsevier

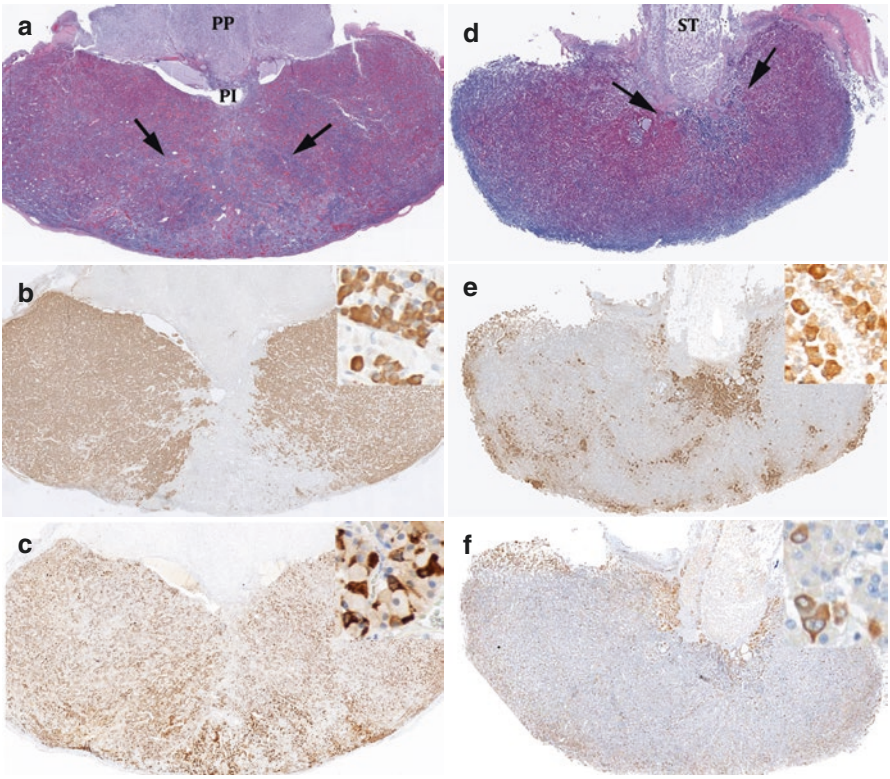

Fig. 2.15 (**a**, **d**) H&E stains of transverse section through an adult male (**a**) and coronal section through a female (**b**) pituitary gland (magnification 15×). Pale staining areas located at the superior surface of the sections correspond to the posterior pituitary (PP) and neural component of the pituitary stalk (ST). Note the high concentration of basophilic cells in the midportion of the pars distalis (below arrows in (**a**, **d**)) comprising the mucoid wedge and in the pars intermedia (PI) in (**a**). (**b**, **c**) Correspond to (**a**) and show the distribution and morphologic appearance of somatotrophs in (**b**) and lactotrophs in (**c**). (**e**, **f**) Correspond to (**d**) and show the distribution and morphologic appearance of corticotrophs (**e**) and gonadotrophs (**f**). Insets ×200. Note tendency for somatotrophs to occupy the lateral wings of the pars distalis and virtual absence from the mucoid wedge, whereas corticotrophs tend to concentrate in the mucoid wedge. A more generalized distribution is seen for lactotrophs and gonadotrophs. Also note particular angularity of lactotrophs compared to other cell types

and thyrotrophs the anteromedial region or mucoid wedge, whereas gonadotrophs are widely dispersed [87]. Each of these cell types is regulated by hypothalamic releasing and inhibitory hormones after they are released into the portal vasculature for conveyance to pars distalis cells (see Lechan and Toni [5] for review).

Corticotrophs are medium-sized cells and contain large, clear, cytoplasmic vacuoles known as "enigmatic bodies" that are lysosomal complexes, easily identified on routine H&E sections. By electron microscopy, numerous secretory granules can be seen along with bundles of intermediate keratin filaments. ACTH immunostaining decorates the cytoplasm of corticotrophs by immunostaining secretory granules, but not keratin filaments or lysosomal bodies [88]. In response to excess glucocorticoids, an accumulation of intermediate filaments results in Crooke's hyaline change in corticotrophs, a pale, pink, glassy, ringlike staining of the cytoplasm on H&E. These changes are readily identified by immunostaining for low-molecular-weight keratins such as CAM5.2 and by demonstrating displacement secretory granules to the cell membrane edges with ACTH antiserum [89]. In cases of extensive Crooke's hyaline change, the keratin filaments will occupy almost the entire cytoplasm, the cells become larger, and the nuclei develop prominent nucleoli.

Somatotrophs comprise the largest cell population of the pars distalis and are round to oval shaped with round nuclei. Immunostaining with GH-directed antibodies shows particularly strong cytoplasmic immunopositivity and the best way to recognize these cells. By electron microscopy, active cells have prominent, lamellar, rough endoplasmic reticulum and large Golgi regions. The entire cytoplasm is filled with dense secretory granules measuring from 150 to 800 nm in diameter, and there is a prominent endoplasmic reticulum that changes with the activity of the cell [90].

Lactotrophs are also well delineated by prolactin antiserum. Ultrastructural morphology identifies cells with both dense and sparse granules, although sparsely granulated cells make up the majority of prolactin-producing cells that actively secrete the hormone. The endoplasmic reticulum is well developed with parallel arrays that can occasionally form concentric structures called the Nebenkern formation. Long cytoplasmic processes can project into the center of acini and wrap around gonadotrophs, providing morphologic evidence suggesting paracrine regulation (see below).

Mammosomatotrophs resemble somatotrophs but produce both growth hormone and prolactin, detected within the same cell by immunohistochemistry and even within the same secretory granule. Two types of mammosomatotrophs have been identified by electron microscopy including cells containing numerous, small electrodense granules (150–400 nm), and cells with large cigar-shaped granules ranging up to 2000 nm with variable density [91].

Thyrotrophs are medium-sized, angulated cells that contain an eccentric nucleus. The cells are filled with small secretory granules that measure 100–200 nm, short rough endoplasmic reticulum and large Golgi complexes.

Gonadotrophs can be bihormonal or contain only one of the gonadotropins. By electron microscopy, round Golgi complexes and numerous granules are characteristic. The size of secretory granules varies in males and females: smaller secretory granules in male and larger secretory granules in females. Gonadotrophs frequently show oncocytic change and squamous metaplasia in older individuals.

Several of the major anterior pituitary cell types can also be detected in the adult pituitary with antiserum directed against transcription factors involved in their embryologic development. Included are TPIT that can be detected in corticotrophs [92], Pit-1 that can be found in somatotrophs, lactotrophs and thyrotrophs [93], steroidogenic factor 1 (SF-1) that is present in gonadotrophs, and GATA-2 in gonadotrophs and thyrotrophs [94]. These transcription factors can be retained in pituitary adenomas, facilitating the identification of their cell type [95]. All anterior pituitary cell types also can be identified with antiserum to the epithelial marker, CAM5.2 (low molecular weight keratin), and to the neuroendocrine marker, synaptophysin. Immunocytochemistry for alpha subunit also identifies cells producing LH, FSH, and TSH, since all are glycoprotein hormones and contain a common alpha subunit.

There are also small populations of other cellular subtypes in the pars distalis. Included are oncocytes that contain abundant mitochondria making the cytoplasm appear eosinophilic and granular by routine H&E stain and become more prominent with aging; null cells that are scattered throughout the pars distalis and, thereby, cannot be classified by hormone production and represent resting or stem cells; and follicular cells that tend to be seen in areas of cell injury or adjacent to tumors, formed from somatotrophs, lactotrophs, and/or corticotrophs that surround damaged cells and become degranulated and dedifferentiated. The folliculostellate cell comprises approximately 5–10% of the pars distalis cell population and is described more fully below.

It is becoming increasingly recognized that the organization of the pars distalis is vastly more complicated than described above. First, there is morphological and physiological evidence for heterogeneity among the classical anterior pituitary cell types including at least three subtypes of somatotrophs (sparsely granulated cell, densely granulated cells, and, as described above, mammosomatotrophs) and functionally different lactotrophs [96–98]. Plurihormonal cells in the human pituitary are also commonly found, particularly for somatotrophs and lactotrophs in which up to 25% of somatotrophs and 15% of lactotrophs co-express FSH [87]. Up to 4% of thyrotrophs co-express FSH, ACTH, or LH [87].

Cell clustering has also been observed for several of the hormonal cell types in the pars distalis and to form networks that can extend distances over the pars distalis [99], presumably as a way to integrate or amplify signals from the hypothalamus. The organization of these networks tends to change with specific phases of development or alterations in physiologic milieu [99, 100], indicative of the plasticity of the pars distalis. For example, during lactation, there is proliferation and reorganization of lactotrophs into a honeycomb-like structure with increased contacts between the cells as a way to coordinate increased output of prolactin [99, 101]. Somatotrophs tend to form clusters that are interconnected by strands of single somatotrophs but become particularly prominent during puberty in association with the growth spurt [100].

In addition to the above, there is strong evidence that the microenvironment of hormonal-secreting cells in the pars distalis is an important component for cell regulation in conjunction with neurosecretion from the hypothalamus. This local, regulatory control mechanism is mediated by paracrine and autocrine secretion of pars distalis hormones utilizing an expanding list of peptides, growth factors, cytokines, binding proteins, gases, and neurotransmitters listed in Table 2.4 (see Denef for

Table 2.4 Nonclassical anterior pituitary substances and cell(s) of origin

Substances	Cell types
Peptides	
Activin B, inhibin, follistatin	F,G
Aldosterone-stimulating factor	UN
Angiotensin II (angiotensinogen, angiotensin I	C,G,L,S
Converting enzyme, cathepsin B, renin)	
Atrial natriuretic peptide	G
AVP	C
Corticotropin-releasing hormone-binding protein	C
Dynorphin	G
Enkephalin	S
Endothelins	L
Galanin	L,S,T
Ghrelin	L,S,T
Gawk (chromogranin B)	G
Growth hormone-releasing hormone	UN
Histidyl-proline diketopiperazine	UN
Motilin	S
Neuromedin B	T
Neuromedin U	C
Neuropeptide Y	S,T
Neurotensin	G,T
Protein 7B2	G,T
Somatostatin 28	UN
Substance P (substance K)	C,L,G,S,T
Thyrotropin-releasing hormone	G,L,S,T
Urocortin	C,L,S
Vasoactive intestinal polypeptide	G,L,T
Growth factors	
Basic fibroblast growth factor	C,F
Chondrocyte growth factor	UN
Epidermal growth factor	G,T
Glial cell-derived neurotrophic factor	F
Insulin-like growth factor I	S,F
Nerve growth factor	L
Pituitary cytotropic factor	UN
Transforming growth factor alpha	l,s,g
Vascular endothelial growth factor	F
Cytokines	
Interleukin-1 beta	T
Interleukin-6	F
Leukemia inhibitory factor	C,F

(continued)

Table 2.4 (continued)

Substances	Cell types
Neurotransmitters	
Acetylcholine	C,L
Nitric oxide	F,G
Other	
Endocannabinoids	C,L,S
Carboxypeptidase E	C,L,S
Carboxypeptidase	D,C
Carboxypeptidase Z	C,G,L,S,T
Leptin	C,F,G,S,T

Modified from Lechan and Toni [5]
C corticotroph, *F* folliculostellate cell, *G* gonadotroph, *L* lactotroph, *S* somatotroph, *T* thyrotroph, *UN* unknown

extensive review [102]). That some gonadotrophs are closely apposed to lactotrophs was first recognized by Nakane [103] and later demonstrated by Denef and Andries [104] that gonadotrophs secrete substances in response to GnRH that stimulate prolactin secretion. Namely, medium from a highly enriched population of gonadotrophs in culture treated with GnRH, when added to a highly enriched population of lactotrophs, induces prolactin secretion [105]. Candidate substances derived from gonadotrophs abound and include pituitary glycoprotein hormone alpha subunit (αGSU), a N-terminal fragment of POMC (POMC 1–74), neurotensin, angiotensin II, PACAP, calcitonin, and CART among a number of other substances [102]. Gonadotrophs may also modulate the secretion from somatotrophs and corticotrophs through paracrine interactions [102]. Autocrine regulation has been recognized for somatotrophs, which express growth hormone receptors [106] that when activated, exert an inhibitory action on its own secretion [106]. Other substances may also contribute to autocrine regulation of somatotrophs including ghrelin, TRH, leptin, enkephalin, NPY, and substance P [102]. Numerous other examples of autocrine control can be found in the literature including evidence that lactotrophs are under autocrine regulation by galanin, VIP may mediate the proliferative response of lactotrophs to estrogen, neuromedin B produced by thyrotrophs exerts an inhibitory effect on TSH secretion, and activin B produced by gonadotrophs selectively induces LH secretion without having an effect on FSH secretion [102].

Paracrine regulation and network functioning are also facilitated by a nonhormonal cell type, the folliculostellate cell. The folliculostellate cell is a small, chromophobic, stellate-shaped cell with long, delicate cytoplasmic processes (Fig. 2.16) creating a meshwork in which the glandular cells of the pars distalis reside [107]. Because they are immunopositive for glial fibrillary acidic protein (GFAP), cytokeratin, vimentin, and fibronectin, they are believed to be of glial origin. Folliculostellate cells are also strongly immunopositive for S-100. These cells function as part of an intrapituitary regulatory center, modulating glandular cells of the pars distalis as an excitable network capable of transmitting signals over long distances by electronic coupling to each other through gap junctions and intercellular junctions (zona adherens) [102, 108]. Folliculostellate cells also make contact with

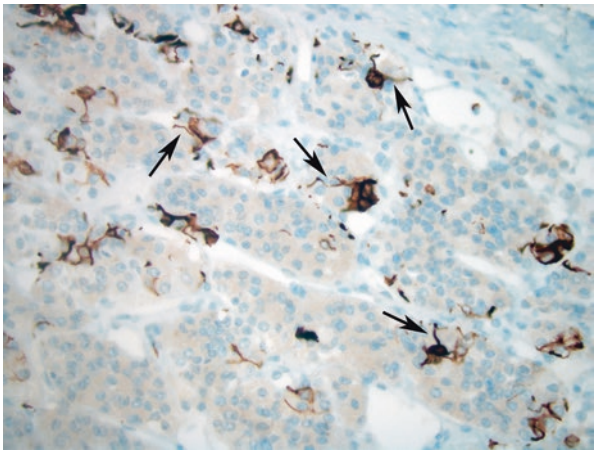

Fig. 2.16 GFAP immunostaining of folliculostellate cells in pars distalis. Note typical stellate appearance highlighted by dark brown cytoplasmic immunopositivity, close association with glandular cells, and long, cytoplasmic processes (arrows) that extend into acini. Magnification ×400

hormonal cells in the pars distalis and, through the release of a variety of substances including cytokines and growth factors listed in Table 2.4, can modify pituitary hormone secretion [100, 102]. Among many examples include a paracrine action of folliculostellate cell-derived IL-6 in response to endotoxin contributing to the increase in ACTH from corticotrophs [109], basic fibroblast growth factor and glial cell-derived neurotrophic factor as permissive for the mitogenic effect of estradiol on lactotrophs [110] and regulation of lactotroph apoptosis [111], respectively, and a role in the luteinizing hormone surge [112]. Folliculostellate cells also contribute to organization of the extracellular matrix surrounding clusters of pars distalis cells by regulating collagen synthesis from pericytes through the release of TGFβ2 [113] and laminin from gonadotrophs [114] and potentially contribute to the stem cell population [115].

Pars Intermedia

The pars intermedia is located between the pars distalis and posterior pituitary, but there is no clearly defined boarder. Although well developed during fetal development in man, it involutes shortly after birth and in the adult consists of clusters of basophil cells (corticotrophs) around colloid-filled cysts in dorsal portions of the mucoid wedge and PAS positive (Figs. 2.15a and 2.17a), but in some cases only scant connective tissue can be found [116]. Here, corticotrophs tend to be smaller than in the pars distalis, have more granules, and are less sensitive to glucocorticoids as they do not develop Crooke's hyaline change and contain fewer keratin filaments. Some of these cells comprise the basophil invasion and extend well into the posterior pituitary (Fig. 2.17b, c), found in approximately 62% of human autopsy series [117]. However, the basophil invasion is more often seen in aging men, although the significance of this phenomenon is unknown and there are no endocrine abnormalities recognized. The pars intermedia is primarily comprised of a

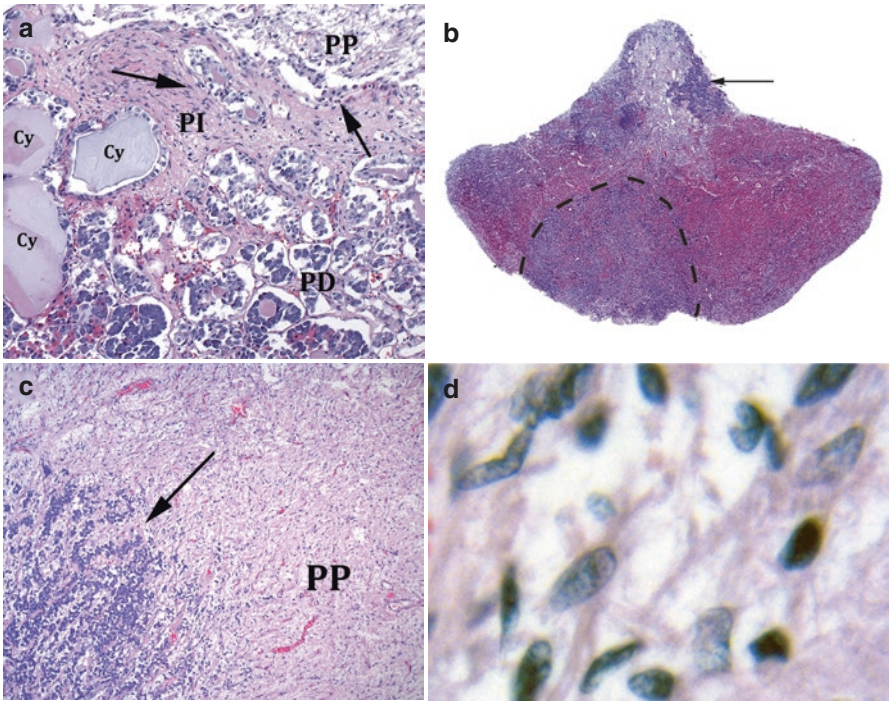

Fig. 2.17 (**a**) H&E stain of the pars intermedia (PI, corresponds to Fig. 2.15a) at the interphase of the pars distalis (PD) and posterior pituitary (PP). The PI contains multiple follicular cysts (Cy) lined with columnar cells and filled with homogeneous, eosinophilic, colloidal material, and areas of basophilic cells (arrows), presumed to be melanotrophs of the PI, interspersed within fibrous tissue. (**b**) H&E stain of an adult male pituitary gland (coronal section) showing the basophil invasion (arrow) into the posterior pituitary. The mucoid wedge is seen below the dotted line and contains mainly basophilic cells. (**c**) Higher magnification of basophil invasion (arrow) and posterior pituitary (PP). The PP is readily recognizable as neural tissue with a fibrillary background and fine capillary network. (**d**) High magnification of a region of the PP shown in (**c**). Note typical appearance of the numerous, spindle-shaped pituicytes. Magnification ×100 in (**a**), ×15 in (**b**), ×200 in (**c**) and ×600 in (**d**)

single cell type that synthesizes pro-opiomelanocortin (POMC), but as opposed to anterior pituitary corticotrophs, these cells do not generally produce ACTH due to extensive processing of the prohormone [118]. Rather, the major peptide contained in pars intermedia cells is α-MSH, and hence, they are commonly referred to as melanotrophs. Extensive processing also results in the production of β-endorphin, but because it is N-acetylated, it does not have opiate activity [118]. Small clusters of ACTH-producing cells have also been identified in the vicinity of the pars intermedia but could also belong to the pars distalis.

As opposed to the pars distalis, the pars intermedia is essentially hypovascular [119, 120], although there is evidence that any secretory products from these cells can reach the peripheral bloodstream via the posterior pituitary vasculature [121]. However, the pars intermedia is directly innervated by axonal fibers originating

from the hypothalamus. Included are dopamine- and serotonin-containing axons [122–124] and TRH-containing axons [125]. Melanotrophs also express dopamine D2 receptors [126] and TRH receptors [125]. The propensity for the pars intermedia to selectively recruit a neuronal innervation may relate to the ability of these cells to express brain-derived neurotrophic factor [127, 128]. While the physiologic significance of this innervation in amphibians is clear, as dopamine inhibits and TRH stimulates the release of α-MSH, allowing α-MSH to regulate pigment dispersion in dermal melanophores [129], the role of the pars intermedia in man is of uncertain physiologic importance. Nevertheless, the common occurrence of the basophil invasion in the posterior pituitary and evidence that these cells also produce α-MSH and have a high proliferative index indicative of active mitosis [117] suggest a potential, functional role for these cells in the adult human brain.

Marginal Zone

Although not considered one of the major subdivisions of the anterior pituitary, the region that comprises the first row of cells from each of the pars distalis and the intermediate lobe is referred to as the marginal zone and is conserved in the human pituitary [130]. The main cell population consists of ciliated epithelial cells that are attached to each other and co-express a variety of stem cell markers such as Sox2, Sox9, Gfra2, RET, Oct 4, SEA4, Prop1, and KLf4 [131]. Tracing experiments indicate that these cells are capable of migrating into the pars distalis and differentiating into mature, hormone-producing cells [132] and may underlie the plasticity of the anterior pituitary in response to physiological changes as discussed previously.

Pars Tuberalis

The pars tuberalis is composed of columns of cells separated by sinuses, very much like the structure of the pars distalis, but encircling the infundibular stem (Fig. 2.6b) and in close contact with the base of the median eminence superiorly and pars distalis inferiorly. The physiological role of the pars tuberalis in man remains somewhat enigmatic, but it is clear that it is part of the photosensing pathway in the CNS and, in some mammals and birds, has an established role in the regulation of seasonal reproduction, sexual behavior, and hibernation (for reviews see Wood and Loudon [133], Korf [134], Azzali et al. [135]). The majority of cells that make up the pars tuberalis (PT-specific cells) are immunoreactive for the common, glycoprotein alpha subunit (CGA) due to the presence of gonadotrophs and thyrotropes [136]. As opposed to thyrotrophs in the pars distalis, however, pars tuberalis thyrotrophs are smaller and lack receptors for TRH [137]. Rather, they express the melatonin MT1 receptor [138, 139], which, in response to melatonin, results in the expression and release of TSH as part of a complex, so-called retrograde pathway

that by increasing type 2 deiodinase activity in third ventricular tanycytes, ultimately leads to the regulation of GnRH secretion in the mediobasal hypothalamus [140, 141]. Melatonin also appears to have an important role in the regulation of clock genes in the pars tuberalis including *Clock*, *Bmal1*, *Per2*, *Cry1*, and *Cry2* [142] that serve to mediate the photoperiodic signal generated by melatonin. Evidence that the pars tuberalis can activate Iκ-Bα in response to endotoxin, indicative of cytokine signaling through the NF-κB pathway, also suggests a role in immune modulation and hypothesized contribute to the mechanism of nonthyroidal illness during infection [143].

The pars tuberalis may also be involved in the seasonal release of prolactin secretion from the pars distalis through an "anterograde pathway" utilizing a variety of other substances including neurokinin A, substance P, and endocannabinoids [134]. In man, the CB1 receptor is most highly expressed in folliculostellate cells and corticotrophs in the pars distalis, however, indicating that any effect of the pars tuberalis on prolactin secretion must be indirect through paracrine regulation in the pars distalis [136]. Given the high expression of CB1 receptors on corticotrophs, the release of endocannabinoids by the pars tuberalis may also contribute to the regulation of the hypothalamic-pituitary-adrenal axis through direct, inhibitory effects in the pars distalis [144, 145].

Posterior Pituitary

The posterior pituitary is the lowest part of a continuous bundle of nerve fibers that extend from the hypothalamic magnocellular neurons that produce vasopressin and oxytocin, pass through the internal layer of the median eminence that forms the base of the hypothalamic infundibulum, and then proceed into the infundibular stem to terminate in the posterior pituitary (see above, Pituitary Anatomy). This bundle is composed of numerous unmyelinated and sparsely myelinated axons and axon terminals containing large neurosecretory vesicles, specialized glial cells called pituicytes, and a rich capillary network (Fig. 2.17c, d). The neurosecretory material is largely made up of the nonapeptides, vasopressin and oxytocin, and their carrier proteins, derived from magnocellular neurons in the hypothalamic paraventricular and supraoptic nuclei, but a variety of other substances are also found in the posterior pituitary, co-contained in vasopressin and oxytocin terminals. Coexisting in vasopressin axon terminals are dynorphin, galanin, pituitary adenylate pituitary cyclase-activating polypeptide (PACAP), secretin, and glutamate and in oxytocin axon terminals, dynorphin and proenkephalin A-derived μ-opioid peptides (see Brown [146] for review). In addition, neurons synthesizing dopamine and norepinephrine originating from the hypothalamus and brainstem, respectively, also innervate the posterior pituitary [147].

The importance of vasopressin as an antidiuretic hormone and oxytocin in uterine contraction and milk letdown is well known. Coexisting substances in vasopressin and oxytocin neurons are presumed to modulate the secretion of vasopressin and

oxytocin from the posterior pituitary and/or their dendritic processes in the hypothalamus [146]. This concept is supported by an inhibitory effect of dynorphin on phasic activity of vasopressin secretion [146] and the existence of kappa opioid receptors, the endogenous ligand for dynorphin, on nerve terminals in the posterior pituitary [148]. However, it is also possible that some substances, such as dopamine, are destined for regulation of the anterior pituitary by way of the short portal vessels [149] that interconnect the capillary beds in the posterior pituitary with the anterior pituitary [150].

Pituicytes comprise approximately 25% of the posterior pituitary and have been classified into parenchymatous and fiber subtypes [151]. Parenchymatous pituicytes are large cells and immunostain with thyroid transcription factor −1 (TTF-1), glial fibrillary acid protein (GFAP), and S100, whereas fibrous pituicytes, the most abundant pituicyte, are small cells and immunostain only with S100 (Fig. 2.17d). The significance of this morphologic distinction is uncertain. However, pituicytes contain processes that interconnect with each other through tight, gap, intermediate, and complex junctions, terminate on blood vessels, and envelop axon terminals containing vasopressin and oxytocin, indicative of an important role in regulating vasopressin and oxytocin secretion [152]. Namely, under basal conditions, pituicytes completely engulf the neurosecretory axon endings and interject their processes between secretory nerve endings and the basal lamina of the fenestrated vasculature. Dehydration, however, results in retraction of pituicyte processes (stellation) from axon terminals and at the vascular surface, favoring increased hormone release into the peripheral bloodstream. Pituicytes are also believed to be osmotic sensors and produce humoral factors such as galanin-like peptide (GALP) in response to hypertonic saline [153], which may contribute to the release of vasopressin and oxytocin from neuronal endings in the posterior pituitary [154]. Conversely, pituicytes release taurine in response to hypotonic conditions, inhibiting hormone release from the posterior pituitary [155]. Thus, as summarized by Rosso and Mienville [156], pituicytes may control neurohormone output by at least two major mechanisms, through structural modifications and by the release of hormone modulators.

Concluding Remarks

The pituitary gland comprises only a tiny fraction of the intracranial volume, yet as apparent from current understanding of its embryologic development, macroscopic and microscopic anatomy, and functionality, it is a highly complicated structure. Particularly exciting is the potential for regeneration of the pars distalis, given evidence for embryonic stem cells in the marginal zone of the pars intermedia and the remarkable plasticity of the adenohypophysis as apparent during adolescent development in women and in association with primary hypothyroidism, pregnancy, and primary hypoadrenalism. Evidence for communication between tanycytes in the hypothalamus and hormonal-producing cells in the pars tuberalis has provided new insights about the functionality of this portion of the anterior pituitary in animal models, but although also

a well-established structure in man, its role is still unknown. While the pituitary has fascinated scientists over the centuries and a vast amount of knowledge has been amassed since the original Galenic concepts, we still have much to learn.

Acknowledgements We wish to thank Fulvio Barbaro, Elia Consolini, Marco Alfieri, and Davide Dallatana, Section of Human Anatomy and Museum BIOMED, University of Parma Parma, Italy, for invaluable help in preparing and photographing the anatomical material on the skull, cranial base, and microvascular anatomy of the human pituitary gland, and Dr. Arthur Tischler, Professor of Pathology, Tufts Medical Center, for his assistance with the histochemical preparations of the anterior pituitary.

References

1. Toni R. The neuroendocrine system: organization and homeostatic role. J Endocrinol Investig. 2004;27:35–47.
2. Joshi BC. Neurology in ancient India: ājñā chakra – a physiological reality. Indian J Hist Sci. 1989;22:292–315.
3. Ray P. Medicine – as it evolved in ancient and mediaeval India. Indian J Hist Sci. 1970;5:86–100.
4. Toni R, Malaguti A, Benfenati F, Martini L. The human hypothalamus: a morpho-functional perspective. J Endocrinol Investig. 2004;27:73–94.
5. Lechan RM, Toni R. Functional anatomy of the hypothalamus and pituitary. 2015/04/24 ed: SourceEndotext [Internet]. South Dartmouth: MDText.com; 2016.
6. Anderson E, Haymaker W. Breakthroughs in hypothalamic and pituitary research. Prog Brain Res. 1974;41:1–60.
7. Haymaker W, Anderson E, Nauta WJH. The hypothalamus. Springfield: Charles C. Thomas; 1969.
8. Iliff JJ, Lee H, Yu M, Feng T, Logan J, Nedergaard M, Benveniste H. Brain-wide pathway for waste clearance captured by contrast-enhanced MRI. J Clin Invest. 2013;123:1299–309.
9. Toni R. Il sistema ipotalamo-ipofisi nell'antichità [The hypothalamic-pituitary system in the antiquity] – Dedicato alla memoria del Prof. Aldo Pinchera [Dedicated to the memory of Prof. Aldo Pinchera]. L'Endocrinologo. 2012;13:1–11.
10. Toni R. Ancient views on the hypothalamic-pituitary-thyroid axis: an historical and epistemological perspective. Pituitary. 2000;3:83–95.
11. Bargmann W. The neurosecretory connection between the hypothalamus and the neurohypophysis. Z Zellforsch Mikrosk Anat. 1949;34:610–34.
12. Umansky F, Nathan H. The lateral wall of the cavernous sinus. With special reference to the nerves related to it. J Neurosurg. 1982;56:228–34.
13. Songtao Q, Yuntao L, Jun P, Chuanping H, Xiaofeng S. Membranous layers of the pituitary gland: histological anatomic study and related clinical issues. Neurosurgery. 2009;64:ons1–9; discussion ons9–10.
14. Rhoton AL Jr. The sellar region. Neurosurgery. 2002;51:S335–74.
15. Patel CR, Fernandez-Miranda JC, Wang WH, Wang EW. Skull base anatomy. Otolaryngol Clin N Am. 2016;49:9–20.
16. Hong GK, Payne SC, Jane JA Jr. Anatomy, physiology, and laboratory evaluation of the pituitary gland. Otolaryngol Clin N Am. 2016;49:21–32.
17. Isolan GR, de Aguiar PH, Laws ER, Strapasson AC, Piltcher O. The implications of microsurgical anatomy for surgical approaches to the sellar region. Pituitary. 2009;12:360–7.
18. Laws ER Jr, Kern EB. Complications of trans-sphenoidal surgery. Clin Neurosurg. 1976;23:401–16.

19. Abele TA, Salzman KL, Harnsberger HR, Glastonbury CM. Craniopharyngeal canal and its spectrum of pathology. AJNR Am J Neuroradiol. 2014;35:772–7.
20. Arey LB. The craniopharyngeal canal reviewed and reinterpreted. Anat Rec. 1950;106:1–16.
21. Cave AJ. The craniopharyngeal canal in man and anthropoids. J Anat. 1931;65:363–7.
22. Amar AP, Weiss MH. Pituitary anatomy and physiology. Neurosurg Clin N Am. 2003;14:11–23, v.
23. Sahni D, Jit I, Harjeet N, Bhansali A. Weight and dimensions of the pituitary in northwestern Indians. Pituitary. 2006;9:19–26.
24. Bergland RM, Ray BS, Torack RM. Anatomical variations in the pituitary gland and adjacent structures in 225 human autopsy cases. J Neurosurg. 1968;28:93–9.
25. Takano K, Utsunomiya H, Ono H, Ohfu M, Okazaki M. Normal development of the pituitary gland: assessment with three-dimensional MR volumetry. AJNR Am J Neuroradiol. 1999;20:312–5.
26. MacMaster FP, Keshavan M, Mirza Y, Carrey N, Upadhyaya AR, El-Sheikh R, Buhagiar CJ, Taormina SP, Boyd C, Lynch M, Rose M, Ivey J, Moore GJ, Rosenberg DR. Development and sexual dimorphism of the pituitary gland. Life Sci. 2007;80:940–4.
27. Peker S, Kurtkaya-Yapicier O, Kilic T, Pamir MN. Microsurgical anatomy of the lateral walls of the pituitary fossa. Acta Neurochir. 2005;147:641–8; discussion 649.
28. Horvath E, Kovacs K. The adenophyophysis. In: Kovacs K, Asa SL, editors. Fuctional endocrine pathology. Cambridge, MA: Blackwell Scientific Publications; 1991. p. 245–81.
29. Stanfield JP. The blood supply of the human pituitary gland. J Anat. 1960;94:257–73.
30. Ceylan S, Anik I, Koc K, Kokturk S, Cine N, Savli H, Sirin G, Sam B, Gazioglu N. Microsurgical anatomy of membranous layers of the pituitary gland and the expression of extracellular matrix collagenous proteins. Acta Neurochir. 2011;153:2435–43; discussion 2443.
31. Baker BL. Cellular composition of the human pituitary pars tuberalis as revealed by immunocytochemistry. Cell Tissue Res. 1977;182:151–63.
32. Melchionna RH, Moore RA. The pharyngeal pituitary gland. Am J Pathol. 1938;14:763–72, 761.
33. Richards SH, Evans IT. The pharyngeal hypophysis and its surgical significance. J Laryngol Otol. 1974;88:937–46.
34. Puy LA, Ciocca DR. Human pharyngeal and sellar pituitary glands: differences and similarities revealed by an immunocytochemical study. J Endocrinol. 1986;108:231–8.
35. McGrath P. Volume and histology of the human pharyngeal hypophysis. Aust N Z J Surg. 1967;37:16–27.
36. Ciocca DR, Puy LA, Stati AO. Identification of seven hormone-producing cell types in the human pharyngeal hypophysis. J Clin Endocrinol Metab. 1985;60:212–6.
37. McGrath P. Vascularity of the environs of the human pharyngeal hypophysis as a possible indication of the mechanism of its control. J Anat. 1972;112:185–93.
38. McGrath P. The trans-sphenoidal vascular route in relation to the human pharyngeal hypophysis. J Anat. 1972;113:383–90.
39. Ciocca DR, Puy LA, Stati AO. Immunocytochemical evidence for the ability of the human pharyngeal hypophysis to respond to change in endocrine feedback. Virchows Arch A Pathol Anat Histopathol. 1985;405:497–502.
40. Xuereb GP, Prichard MM, Daniel PM. The arterial supply and venous drainage of the human hypophysis cerebri. Q J Exp Physiol Cogn Med Sci. 1954;39:199–217.
41. Leclercq TA, Grisoli F. Arterial blood supply of the normal human pituitary gland. An anatomical study. J Neurosurg. 1983;58:678–81.
42. McConnell EM. The arterial blood supply of the human hypophysis cerebri. Anat Rec. 1953;115:175–203.
43. Xuereb GP, Prichard ML, Daniel PM. The hypophysial portal system of vessels in man. Q J Exp Physiol Cogn Med Sci. 1954;39:219–30.
44. Green HT. The venous drainage of the human hypophysis cerebri. Am J Anat. 1957;100:435–69.

45. Gilbert MS. Some factors influencing the early development of the mammalian hypophysis. Anat Rec. 1935;62:337–57.
46. Saint-Jeannet JP, Moody SA. Establishing the pre-placodal region and breaking it into placodes with distinct identities. Dev Biol. 2014;389:13–27.
47. Takor TT, Pearse AG. Neuroectodermal origin of avian hypothalamo-hypophyseal complex: the role of the ventral neural ridge. J Embryol Exp Morphol. 1975;34:311–25.
48. Ravera S, Morigi FP, Coiro M, Della Casa C, Bondi A, Toni R. Chromogranin A as an early marker of neuroendocrine differentiation in the human embryo: evidence for feasibility of the "triune information network" concept on man. It J Anat Embriol. 2005;110:275.
49. Toni R. A new perspective in neuroendocrine integration: the triune information network (TIN) concept. Proceedings of the First Meeting of the Indian Subcontinent Branch of the International Neuropeptide Society:7–8. 2008
50. Ikeda H, Suzuki J, Sasano N, Niizuma H. The development and morphogenesis of the human pituitary gland. Anat Embryol (Berl). 1988;178:327–36.
51. O'Rahilly R, Muller F. The development of the neural crest in the human. J Anat. 2007;211:335–51.
52. Espinasse PG. The development of the hypophysio-portal system in man. J Anat. 1933;268:11–8.
53. De Beer GR, editor. The development of the vertebrate skull. London: Oxford University Press; 1937.
54. Boyd JD. Observations on the human pharyngeal hypophysis. J Endocrinol. 1956;14:66–77.
55. McGrath P. Aspects of the human pharyngeal hypophysis in normal and anencephalic fetuses and neonates and their possible significance in the mechanism of its control. J Anat. 1978;127:65–81.
56. Baker RC, Edwards LF. Early development of the human pharyngeal hypophysis – a preliminary report. Ohio J Sci. 1948;48:241–5.
57. Pilavdzic D, Kovacs K, Asa SL. Pituitary morphology in anencephalic human fetuses. Neuroendocrinology. 1997;65:164–72.
58. Asa SL, Ezzat S. Molecular determinants of pituitary cytodifferentiation. Pituitary. 1999;1:159–68.
59. Bazina M, Vukojevic K, Roje D, Saraga-Babic M. Influence of growth and transcriptional factors, and signaling molecules on early human pituitary development. J Mol Histol. 2009;40:277–86.
60. Kelberman D, Rizzoti K, Lovell-Badge R, Robinson IC, Dattani MT. Genetic regulation of pituitary gland development in human and mouse. Endocr Rev. 2009;30:790–829.
61. Fang Q, George AS, Brinkmeier ML, Mortensen AH, Gergics P, Cheung LY, Daly AZ, Ajmal A, Perez Millan MI, Ozel AB, Kitzman JO, Mills RE, Li JZ, Camper SA. Genetics of combined pituitary hormone deficiency: roadmap into the genome era. Endocr Rev. 2016;37:636–75.
62. McCabe MJ, Dattani MT. Genetic aspects of hypothalamic and pituitary gland development. Handb Clin Neurol. 2014;124:3–15.
63. Drouin J. Pituitary development. In: Melmed S, editor. The pituitary. 4th ed. San Diego: Academic; 2017. p. 3–22.
64. Cote M, Salzman KL, Sorour M, Couldwell WT. Normal dimensions of the posterior pituitary bright spot on magnetic resonance imaging. J Neurosurg. 2014;120:357–62.
65. Kilday JP, Laughlin S, Urbach S, Bouffet E, Bartels U. Diabetes insipidus in pediatric germinomas of the suprasellar region: characteristic features and significance of the pituitary bright spot. J Neuro-Oncol. 2015;121:167–75.
66. Bonneville F, Cattin F, Marsot-Dupuch K, Dormont D, Bonneville JF, Chiras J. T1 signal hyperintensity in the sellar region: spectrum of findings. Radiographics. 2006;26:93–113.
67. Robertson GL. Diabetes insipidus: differential diagnosis and management. Best Pract Res Clin Endocrinol Metab. 2016;30:205–18.
68. Pecina HI, Pecina TC, Vyroubal V, Kruljac I, Slaus M. Age and sex related differences in normal pituitary gland and fossa volumes. Front Biosci (Elite Ed). 2017;9:204–13.

69. Lurie SN, Doraiswamy PM, Husain MM, Boyko OB, Ellinwood EH Jr, Figiel GS, Krishnan KR. In vivo assessment of pituitary gland volume with magnetic resonance imaging: the effect of age. J Clin Endocrinol Metab. 1990;71:505–8.
70. Doraiswamy PM, Potts JM, Axelson DA, Husain MM, Lurie SN, Na C, Escalona PR, McDonald WM, Figiel GS, Ellinwood EH Jr, et al. MR assessment of pituitary gland morphology in healthy volunteers: age- and gender-related differences. AJNR Am J Neuroradiol. 1992;13:1295–9.
71. Terano T, Seya A, Tamura Y, Yoshida S, Hirayama T. Characteristics of the pituitary gland in elderly subjects from magnetic resonance images: relationship to pituitary hormone secretion. Clin Endocrinol. 1996;45:273–9.
72. Fink AM, Vidmar S, Kumbla S, Pedreira CC, Kanumakala S, Williams C, Carlin JB, Cameron FJ. Age-related pituitary volumes in prepubertal children with normal endocrine function: volumetric magnetic resonance data. J Clin Endocrinol Metab. 2005;90:3274–8.
73. Elster AD. Modern imaging of the pituitary. Radiology. 1993;187:1–14.
74. Castillo M. Pituitary gland: development, normal appearances, and magnetic resonance imaging protocols. Top Magn Reson Imaging. 2005;16:259–68.
75. Dinc H, Esen F, Demirci A, Sari A, Resit Gumele H. Pituitary dimensions and volume measurements in pregnancy and postpartum. MR assessment. Acta Radiol. 1998;39:64–9.
76. Foyouzi N, Frisbaek Y, Norwitz ER. Pituitary gland and pregnancy. Obstet Gynecol Clin N Am. 2004;31:873–92, xi.
77. Axelson DA, Doraiswamy PM, Boyko OB, Rodrigo Escalona P, McDonald WM, Ritchie JC, Patterson LJ, Ellinwood EH Jr, Nemeroff CB, Krishnan KR. In vivo assessment of pituitary volume with magnetic resonance imaging and systematic stereology: relationship to dexamethasone suppression test results in patients. Psychiatry Res. 1992;44:63–70.
78. Mineura K, Goto T, Yoneya M, Kowada M, Tamakawa Y, Kagaya H. Pituitary enlargement associated with Addison's disease. Clin Radiol. 1987;38:435–7.
79. Soni BK, Joish UK, Sahni H, George RA, Sivasankar R, Aggarwal R. A comparative study of pituitary volume variations in MRI in acute onset of psychiatric conditions. J Clin Diagn Res. 2017;11:TC01–4.
80. Ramji S, Touska P, Rich P, MacKinnon AD. Normal neuroanatomical variants that may be misinterpreted as disease entities. Clin Radiol. 2017;72:810–25.
81. Satogami N, Miki Y, Koyama T, Kataoka M, Togashi K. Normal pituitary stalk: high-resolution MR imaging at 3T. AJNR Am J Neuroradiol. 2010;31:355–9.
82. Ahmadi H, Larsson EM, Jinkins JR. Normal pituitary gland: coronal MR imaging of infundibular tilt. Radiology. 1990;177:389–92.
83. Yuh WT, Fisher DJ, Nguyen HD, Tali ET, Gao F, Simonson TM, Schlechte JA. Sequential MR enhancement pattern in normal pituitary gland and in pituitary adenoma. AJNR Am J Neuroradiol. 1994;15:101–8.
84. Rai AR, Rai R, Pc V, Vadgaonkar R, Tonse M. A cephalometric analysis on magnitudes and shape of Sella Turcica. J Craniofac Surg. 2016;27:1317–20.
85. Wang H, Hou B, Lu L, Feng M, Zang J, Yao S, Feng F, Wang R, Li F, Zhu Z. PET/MR imaging in the diagnosis of hormone-producing pituitary micro-adenoma: a prospective pilot study. J Nucl Med. 2017;59:523–8.
86. Wong AO, Ng S, Lee EK, Leung RC, Ho WK. Somatostatin inhibits (d-Arg6, Pro9-NEt) salmon gonadotropin-releasing hormone- and dopamine D1-stimulated growth hormone release from perifused pituitary cells of Chinese grass carp, Ctenopharyngodon idellus. Gen Comp Endocrinol. 1998;110:29–45.
87. Mitrofanova LB, Konovalov PV, Krylova JS, Polyakova VO, Kvetnoy IM. Plurihormonal cells of normal anterior pituitary: facts and conclusions. Oncotarget. 2017;8:29282–99.
88. Neumann PE, Horoupian DS, Goldman JE, Hess MA. Cytoplasmic filaments of Crooke's hyaline change belong to the cytokeratin class. An immunocytochemical and ultrastructural study. Am J Pathol. 1984;116:214–22.
89. Mete O, Asa SL. Clinicopathological correlations in pituitary adenomas. Brain Pathol. 2012;22:443–53.

90. Horvath E, Kovacs K. Fine structural cytology of the adenohypophysis in rat and man. J Electron Microsc Tech. 1988;8:401–32.
91. Losinski NE, Horvath E, Kovacs K, Asa SL. Immunoelectron microscopic evidence of mammosomatotrophs in human adult and fetal adenohypophyses, rat adenohypophyses and human and rat pituitary adenomas. Anat Anz. 1991;172:11–6.
92. Sjostedt E, Bollerslev J, Mulder J, Lindskog C, Ponten F, Casar-Borota O. A specific antibody to detect transcription factor T-Pit: a reliable marker of corticotroph cell differentiation and a tool to improve the classification of pituitary neuroendocrine tumours. Acta Neuropathol. 2017;134:675–7.
93. Lloyd RV, Osamura RY. Transcription factors in normal and neoplastic pituitary tissues. Microsc Res Tech. 1997;39:168–81.
94. Lee M, Marinoni I, Irmler M, Psaras T, Honegger JB, Beschorner R, Anastasov N, Beckers J, Theodoropoulou M, Roncaroli F, Pellegata NS. Transcriptome analysis of MENX-associated rat pituitary adenomas identifies novel molecular mechanisms involved in the pathogenesis of human pituitary gonadotroph adenomas. Acta Neuropathol. 2013;126:137–50.
95. McDonald WC, Banerji N, McDonald KN, Ho B, Macias V, Kajdacsy-Balla A. Steroidogenic factor 1, Pit-1, and adrenocorticotropic hormone: a rational starting place for the immunohistochemical characterization of pituitary adenoma. Arch Pathol Lab Med. 2017;141:104–12.
96. Snyder G, Hymer WC, Snyder J. Functional heterogeneity in somatotrophs isolated from the rat anterior pituitary. Endocrinology. 1977;101:788–99.
97. Nikitovitch-Winer MB, Atkin J, Maley BE. Colocalization of prolactin and growth hormone within specific adenohypophyseal cells in male, female, and lactating female rats. Endocrinology. 1987;121:625–30.
98. Frawley LS, Clark CL, Schoderbek WE, Hoeffler JP, Boockfor FR. A novel bioassay for lactogenic activity: demonstration that prolactin cells differ from one another in bio- and immuno-potencies of secreted hormone. Endocrinology. 1986;119:2867–9.
99. Le Tissier P, Campos P, Lafont C, Romano N, Hodson DJ, Mollard P. An updated view of hypothalamic-vascular-pituitary unit function and plasticity. Nat Rev Endocrinol. 2017;13:257–67.
100. Le Tissier PR, Hodson DJ, Lafont C, Fontanaud P, Schaeffer M, Mollard P. Anterior pituitary cell networks. Front Neuroendocrinol. 2012;33:252–66.
101. Hodson DJ, Molino F, Fontanaud P, Bonnefont X, Mollard P. Investigating and modelling pituitary endocrine network function. J Neuroendocrinol. 2010;22:1217–25.
102. Denef C. Paracrinicity: the story of 30 years of cellular pituitary crosstalk. J Neuroendocrinol. 2008;20:1–70.
103. Nakane PK. Classifications of anterior pituitary cell types with immunoenzyme histochemistry. J Histochem Cytochem. 1970;18:9–20.
104. Denef C, Andries M. Evidence for paracrine interaction between gonadotrophs and lactotrophs in pituitary cell aggregates. Endocrinology. 1983;112:813–22.
105. Van Bael A, Vande Vijver V, Devreese B, Van Beeumen J, Denef C. N-terminal 10- and 12-kDa POMC fragments stimulate differentiation of lactotrophs. Peptides. 1996;17:1219–28.
106. Fraser RA, Siminoski K, Harvey S. Growth hormone receptor gene: novel expression in pituitary tissue. J Endocrinol. 1991;128:R9–11.
107. Devnath S, Inoue K. An insight to pituitary folliculo-stellate cells. J Neuroendocrinol. 2008;20:687–91.
108. Vitale ML, Garcia CJ, Akpovi CD, Pelletier RM. Distinctive actions of connexin 46 and connexin 50 in anterior pituitary folliculostellate cells. PLoS One. 2017;12:e0182495.
109. Arzt E, Pereda MP, Castro CP, Pagotto U, Renner U, Stalla GK. Pathophysiological role of the cytokine network in the anterior pituitary gland. Front Neuroendocrinol. 1999;20:71–95.
110. Hentges S, Boyadjieva N, Sarkar DK. Transforming growth factor-beta3 stimulates lactotrope cell growth by increasing basic fibroblast growth factor from folliculo-stellate cells. Endocrinology. 2000;141:859–67.

111. Guillou A, Romano N, Bonnefont X, Le Tissier P, Mollard P, Martin AO. Modulation of the tyrosine kinase receptor Ret/glial cell-derived neurotrophic factor (GDNF) signaling: a new player in reproduction induced anterior pituitary plasticity? Endocrinology. 2011;152:515–25.
112. Lyles D, Tien JH, McCobb DP, Zeeman ML. Pituitary network connectivity as a mechanism for the luteinising hormone surge. J Neuroendocrinol. 2010;22:1267–78.
113. Tsukada T, Azuma M, Horiguchi K, Fujiwara K, Kouki T, Kikuchi M, Yashiro T. Folliculostellate cell interacts with pericyte via TGFbeta2 in rat anterior pituitary. J Endocrinol. 2016;229:159–70.
114. Tsukada T, Fujiwara K, Horiguchi K, Azuma M, Ramadhani D, Tofrizal A, Batchuluun K, Maliza R, Syaidah R, Kikuchi M, Yashiro T. Folliculostellate cells are required for laminin release from gonadotrophs in rat anterior pituitary. Acta Histochem Cytochem. 2014;47:239–45.
115. Rizzoti K. Adult pituitary progenitors/stem cells: from in vitro characterization to in vivo function. Eur J Neurosci. 2010;32:2053–62.
116. Saland LC. The mammalian pituitary intermediate lobe: an update on innervation and regulation. Brain Res Bull. 2001;54:587–93.
117. Fan X, Olson SJ, Johnson MD. Immunohistochemical localization and comparison of carboxypeptidases D, E, and Z, alpha-MSH, ACTH, and MIB-1 between human anterior and corticotroph cell "basophil invasion" of the posterior pituitary. J Histochem Cytochem. 2001;49:783–90.
118. Bicknell AB. The tissue-specific processing of pro-opiomelanocortin. J Neuroendocrinol. 2008;20:692–9.
119. Daikoku S, Kawano H, Abe K, Yoshinaga K. Topographical appearance of adenohypophysial cells with special reference to the development of the portal system. Arch Histol Jpn. 1981;44:103–16.
120. Szabo K, Csanyi K. The vascular architecture of the developing pituitary-median eminence complex in the rat. Cell Tissue Res. 1982;224:563–77.
121. Lamacz M, Tonon MC, Louiset E, Cazin L, Vaudry H. The intermediate lobe of the pituitary, model of neuroendocrine communication. Arch Int Physiol Biochim Biophys. 1991;99:205–19.
122. Goudreau JL, Lindley SE, Lookingland KJ, Moore KE. Evidence that hypothalamic periventricular dopamine neurons innervate the intermediate lobe of the rat pituitary. Neuroendocrinology. 1992;56:100–5.
123. Makarenko IG, Ugrumov MV, Calas A. Axonal projections from the hypothalamus to the pituitary intermediate lobe in rats during ontogenesis: DiI tracing study. Brain Res Dev Brain Res. 2005;155:117–26.
124. Palkovits M, Mezey E, Chiueh CG, Krieger DT, Gallatz K, Brownstein MJ. Serotonin-containing elements of the rat pituitary intermediate lobe. Neuroendocrinology. 1986;42:522–5.
125. Galas L, Raoult E, Tonon MC, Okada R, Jenks BG, Castano JP, Kikuyama S, Malagon M, Roubos EW, Vaudry H. TRH acts as a multifunctional hypophysiotropic factor in vertebrates. Gen Comp Endocrinol. 2009;164:40–50.
126. Pivonello R, Waaijers M, Kros JM, Pivonello C, de Angelis C, Cozzolino A, Colao A, Lamberts SWJ, Hofland LJ. Dopamine D2 receptor expression in the corticotroph cells of the human normal pituitary gland. Endocrine. 2017;57:314–25.
127. Hopker VH, Kjaer B, Varon S. Dopaminergic regulation of BDNF content in the pituitary intermediate lobe. Neuroreport. 1997;8:1089–93.
128. Nakakura T, Suzuki M, Watanabe Y, Tanaka S. Possible involvement of brain-derived neurotrophic factor (BDNF) in the innervation of dopaminergic neurons from the rat periventricular nucleus to the pars intermedia. Zool Sci. 2007;24:1086–93.
129. Hadley ME, Davis MD, Morgan CM. Cellular control of melanocyte stimulating hormone secretion. Front Horm Res. 1977;4:94–104.

130. Garcia-Lavandeira M, Quereda V, Flores I, Saez C, Diaz-Rodriguez E, Japon MA, Ryan AK, Blasco MA, Dieguez C, Malumbres M, Alvarez CV. A GRFa2/Prop1/stem (GPS) cell niche in the pituitary. PLoS One. 2009;4:e4815.
131. Garcia-Lavandeira M, Diaz-Rodriguez E, Bahar D, Garcia-Rendueles AR, Rodrigues JS, Dieguez C, Alvarez CV. Pituitary cell turnover: from adult stem cell recruitment through differentiation to death. Neuroendocrinology. 2015;101:175–92.
132. Rizzoti K, Akiyama H, Lovell-Badge R. Mobilized adult pituitary stem cells contribute to endocrine regeneration in response to physiological demand. Cell Stem Cell. 2013;13:419–32.
133. Wood S, Loudon A. The pars tuberalis: the site of the circannual clock in mammals? Gen Comp Endocrinol. 2017;27:95–112.
134. Korf HW. Signaling pathways to and from the hypophysial pars tuberalis, an important center for the control of seasonal rhythms. Gen Comp Endocrinol. 2017;258:236–43.
135. Azzali G, Arcari ML, Cacchioli A, Toni R. Fine structure and photoperiodical seasonal changes in Pars tuberalis of hibernating bats. Ital J Anat Embryol. 2003;108:49–64.
136. Yasuo S, Unfried C, Kettner M, Geisslinger G, Korf HW. Localization of an endocannabinoid system in the hypophysial pars tuberalis and pars distalis of man. Cell Tissue Res. 2010;342:273–81.
137. Bockmann J, Bockers TM, Winter C, Wittkowski W, Winterhoff H, Deufel T, Kreutz MR. Thyrotropin expression in hypophyseal pars tuberalis-specific cells is 3,5,3′-triiodothyronine, thyrotropin-releasing hormone, and pit-1 independent. Endocrinology. 1997;138:1019–28.
138. Lacoste B, Angeloni D, Dominguez-Lopez S, Calderoni S, Mauro A, Fraschini F, Descarries L, Gobbi G. Anatomical and cellular localization of melatonin MT1 and MT2 receptors in the adult rat brain. J Pineal Res. 2015;58:397–417.
139. Klosen P, Bienvenu C, Demarteau O, Dardente H, Guerrero H, Pevet P, Masson-Pevet M. The mt1 melatonin receptor and RORbeta receptor are co-localized in specific TSH-immunoreactive cells in the pars tuberalis of the rat pituitary. J Histochem Cytochem. 2002;50:1647–57.
140. Hanon EA, Routledge K, Dardente H, Masson-Pevet M, Morgan PJ, Hazlerigg DG. Effect of photoperiod on the thyroid-stimulating hormone neuroendocrine system in the European hamster (*Cricetus cricetus*). J Neuroendocrinol. 2010;22:51–5.
141. Yamamura T, Yasuo S, Hirunagi K, Ebihara S, Yoshimura T. T(3) implantation mimics photoperiodically reduced encasement of nerve terminals by glial processes in the median eminence of Japanese quail. Cell Tissue Res. 2006;324:175–9.
142. Dupre SM. Encoding and decoding photoperiod in the mammalian pars tuberalis. Neuroendocrinology. 2011;94:101–12.
143. Sanchez E, Singru PS, Wittmann G, Nouriel SS, Barrett P, Fekete C, Lechan RM. Contribution of TNF-alpha and nuclear factor-kappaB signaling to type 2 iodothyronine deiodinase activation in the mediobasal hypothalamus after lipopolysaccharide administration. Endocrinology. 2010;151:3827–35.
144. Cota D. The role of the endocannabinoid system in the regulation of hypothalamic-pituitary-adrenal axis activity. J Neuroendocrinol. 2008;20(Suppl 1):35–8.
145. Jafarpour A, Dehghani F, Korf HW. Identification of an endocannabinoid system in the rat pars tuberalis-a possible interface in the hypothalamic-pituitary-adrenal system? Cell Tissue Res. 2017;368:115–23.
146. Brown CH. Magnocellular neurons and posterior pituitary function. Compr Physiol. 2016;6:1701–41.
147. Garten LL, Sofroniew MV, Dyball RE. A direct catecholaminergic projection from the brainstem to the neurohypophysis of the rat. Neuroscience. 1989;33:149–55.
148. Shuster SJ, Riedl M, Li X, Vulchanova L, Elde R. The kappa opioid receptor and dynorphin co-localize in vasopressin magnocellular neurosecretory neurons in guinea-pig hypothalamus. Neuroscience. 2000;96:373–83.

149. Peters LL, Hoefer MT, Ben-Jonathan N. The posterior pituitary: regulation of anterior pituitary prolactin secretion. Science. 1981;213:659–61.
150. Gross PM, Joneja MG, Pang JJ, Polischuk TM, Shaver SW, Wainman DS. Topography of short portal vessels in the rat pituitary gland: a scanning electron-microscopic and morphometric study of corrosion cast replicas. Cell Tissue Res. 1993;272:79–88.
151. Wei XY, Zhao CH, Liu YY, Wang YZ, Ju G. Immuohistochemical markers for pituicyte. Neurosci Lett. 2009;465:27–30.
152. Hatton GI. Pituicytes, glia and control of terminal secretion. J Exp Biol. 1988;139:67–79.
153. Kawasaki M, Saito J, Hashimoto H, Suzuki H, Otsubo H, Fujihara H, Ohnishi H, Nakamura T, Ueta Y. Induction of the galanin-like peptide gene expression in the posterior pituitary gland after acute osmotic stimulus in rats. Neurosci Lett. 2007;419:125–30.
154. Onaka T, Kuramochi M, Saito J, Ueta Y, Yada T. Galanin-like peptide stimulates vasopressin, oxytocin and adrenocorticotropic hormone release in rats. Neuroreport. 2005;16:243–7.
155. Hussy N. Glial cells in the hypothalamo-neurohypophysial system: key elements of the regulation of neuronal electrical and secretory activity. Prog Brain Res. 2002;139:95–112.
156. Rosso L, Mienville JM. Pituicyte modulation of neurohormone output. Glia. 2009;57:235–43.
157. O'Malley CD, de CM Saunders JB. Leonardo on the human body. New York: Dover Publications; 1983.
158. Meshberger FL. An interpretation of Michelangelo's creation of Adam based on neuroanatomy. JAMA. 1990;264:1837–41.
159. Di Iorgi N, Morana G, Allegri AE, Napoli F, Gastaldi R, Calcagno A, Patti G, Loche S, Maghnie M. Classical and non-classical causes of GH deficiency in the paediatric age. Best Pract Res Clin Endocrinol Metab. 2016;30:705–36.
160. Giordano M. Genetic causes of isolated and combined pituitary hormone deficiency. Best Pract Res Clin Endocrinol Metab. 2016;30:679–91.